Disruption risk mitigation in intermodal rail-truck transportation of hazardous materials

DISRUPTION RISK MITIGATION VIA OPTIMIZATION AND MACHINE LEARNING IN RAIL-TRUCK INTERMODAL TRANSPORTATION OF HAZARDOUS MATERIALS

BY

ARASH MORADI RAD

A THESIS

SUBMITTED TO THE SCHOOL OF COMPUTATIONAL SCIENCE AND ENGINEERING

AND THE SCHOOL OF GRADUATE STUDIES

OF MCMASTER UNIVERSITY

IN PARTIAL FULFILLMENT OF THE REQUIREMENTS

FOR THE DEGREE OF

MASTER OF SCIENCE

© Copyright by Arash Moradi Rad, October 2020

All Rights Reserved

Master of Science (2020) McMaster University

Computational Science and Engineering Hamilton, Ontario, Canada

TITLE: Disruption risk mitigation via optimization and machine learning in rail-truck intermodal transportation of hazardous materials

AUTHOR: Arash Moradi Rad

SUPERVISOR: Dr. Manish Verma

NUMBER OF PAGES: xi, 114

Abstract

Random disruptions resulting in loss of functionality in service legs or intermodal terminals of transportation networks are an inevitable part of operations, and considering the crucial role of aforementioned networks, it is prudent to strive towards avoiding high-consequence disruption events. The magnitude of the negative impact of a disruption is dependent on component criticality; therefore, limited resources of disruption mitigation should be assigned to the infrastructure with the highest priority. However, categorizing the service legs and terminals based on their actual post-disruption impact is computationally heavy and inefficient. We propose a methodology based on the combination of a bi-objective hazmat shipment planning optimization model and machine learning to identify critical infrastructure more efficiently. The proposed methodology is applied to part of CSX Corporation's intermodal rail-truck network in the United States as a realistic size problem instance, in order to gain managerial insight and to evaluate the performance of the methodology.

Acknowledgments

I will feel forever grateful to my dearest supervisor, Dr. Manish Verma for his support, guidance, patience and fatherly care throughout my graduate studies. I would like to sincerely thank him for providing me with this wonderful opportunity to learn, grow and expand my horizons which would not have been otherwise possible.

I would also like to thank my thesis examination committee members, Dr. Yun Zhou and Dr. Kai Huang for taking the time to review my thesis.

Many thanks to my professors, colleagues and dear friends at McMaster University for making these past two years an amazing and memorable journey.

Last but not least, I would like to express my love and gratitude to my mother who is the kindest person I have ever known and who has sacrificed so much to create a better life for her children.

Contents

List of Tables

List of Figures

Chapter 1

Introduction

Hazardous materials (hazmat) are defined by the Pipeline and Hazardous Materials Safety Administration of the U.S. Department of Transportation as chemicals or substances that can potentially cause a highly significant risk to health and safety of the surrounding population and property during commercial transportation (PHMSA, 2020a). This definition underlines the potential health and physical harms and hazards associated with transportation of hazmat such as crude oil or combustible/flammable liquids; however, these chemicals are essential to the sustenance and growth of today's industrial economies and therefore, there is a significant demand for their transportation from manufacturing plants to consumers.

Although a multitude of regulations and initiatives have been undertaken and comprehensive safety plans have been implemented to reduce the likeli-

hood of accidents involving the release of hazmat, on average approximately 10 fatalities and 143 injuries per year have been caused by accidents involving hazardous materials on United States highways between 2010 and 2019 (PHMSA, 2020b). For instance, in June 2015, a truck carrying diesel fuel was involved in an accident in South Carolina that resulted in the spillage and ignition of hazmat cargo causing three fatalities and one case of serious injury (PHMSA, 2020b). When it comes to hazmat transportation risk, railroads are among the safest modes; nonetheless, multicar incidents and the resulting catastrophes still occur on rare occasions (Verma & Verter, 2013). A recent example of such a catastrophe resulting from the rail transportation of hazmat freight is the Lac-Mégantic rail disaster that happened in Quebec, Canada on July 5, 2013.(TSB, 2019). Catastrophic incidents such as the above-mentioned tragic incidents in both the rail and truck modes of transportation highlight the necessity of including risk-cost tradeoffs into routing decisions and the incorporation of hazmat risk assessment methodologies that accurately capture the damage caused by an accident involving the release of hazmat for the exposed population.

One of the factors that significantly affects routing decisions and the consequent transport risk is the choice of transportation mode. Although most of the hazardous material shipments were carried by a single mode in the United States, 27.3 million tons of hazmat were transported via a combina-

tion of modes accounting for 10.4 percent of total ton-miles in 2012 (BTS, 2017). This can be attributed to the fact that many industries that process hazardous materials do not have the dedicated industrial rail tracks needed for direct delivery. Consequently, utilizing a combination of rail and highway transportation presents itself as a viable and valuable option for them.

Rail-truck intermodal i.e. the transportation of containers by a combination of rail and truck, has experienced a steady and significant growth over the past thirty years. The rising interest in intermodal rail-truck transportation stems from global supply chain requirements and several other factors. It provides customers with the opportunity to take advantage of both the highway and rail transportation modes and hence, a more cost-effective and efficient movement of their freight. The rise in standard container utilization, as evidenced by the fact that in 1990, containers accounted for 47 percent of intermodal volume which rose to 69 percent at the turn of the century in 2000, and a record 92 percent in 2017, has also been another contributing factor since unlike trailers, containers can be double stacked which leads to increased productivity as well as cost competitiveness and ease of transfer between various modes (AAR, 2018a). Furthermore, uncertainty in lead-times will decrease since a notable portion of freight movement is performed by reliable and punctual trains operating on predetermined schedules (Nozick & Morlok, 1997).

Moreover, the future and growth of the intermodal transportation industry appears to be highly promising. According to the Association of American Railroads, 5.6 million containers and trailers were moved in the US rail-truck intermodal network in 1990, and this volume has grown to 9 million containers in 2000, to 11.1 million in 2010, culminating in a record 14.5 million units in 2018 (AAR, 2018a). Furthermore, the Association of American Railroads reports that between 2000 and 2017, there has been a 52.2 percent increase in rail intermodal volumes (AAR, 2018b). According to the estimates of the Freight Analysis Framework (FAF) which is a data set comprising the records of all freight movements within the United States, the total value of shipments transported via multiple modes will increase from 3.3 trillion dollars in 2016 to nearly 9 trillion dollars in 2045, signifying a growth of more than two and a half times in the mentioned time period (BTS & FHWA, 2018).

The magnitude of the volumes of both hazmat and regular freight being transported on the intermodal networks and the crucial role they play in the economic sustenance and growth of North America, highlight the importance and criticality of the underlying infrastructure. In other words, the intermodal terminals, rail tracks and roads can be considered critical infrastructure both for the United States economy as a whole, and for the intermodal transportation companies as evidenced by the fact that 24 percent of the revenue generated by U.S. Class 1 railroad operators in 2018 was accounted for

by intermodal shipments which is the highest percentage among all the single product groups and much higher than coal that used to be the most significant source of transport revenue for these major railroad operators (AAR, 2018a).

The importance of these infrastructure for intermodal transportation companies highlights the need for incorporating measures in the company's contingency plans to manage the risk of random disruptions resulting in the loss of functionality in a network element. It is worthy to note that railroad operations are disrupted far more regularly when compared to business operations (Stecke & Kumar, 2009). Intermodal terminals may either be disrupted by random events like natural disasters, crane technical failures or by intentional attacks (Sarhadi et al., 2017); whereas rail tracks may be disrupted by natural disasters or by rail track deterioration, etc. A recent example of disruptions in railroad operations is the rail blockades across Canada due to protests which significantly hampered the ability of railroad companies to transport goods and passengers (CBC, 2020). Hence, the need for a framework that assists decision makers in creating superior contingency plans that would lessen the severity of a random disruption event's consequences becomes evident.

This study investigates the possibility of developing disruption risk mitigation strategies based on the knowledge of most critical train service legs and intermodal terminals in a network, obtained via predictive analytics in rail-

truck intermodal transportation of hazmat and regular freight. We propose a methodology that utilizes machine learning techniques and mathematical optimization to more efficiently identify the most critical infrastructure in terms of the impact of disruption, so as to assist decision makers in the development and implementation of mitigation strategies. The proposed methodology is ultimately applied to a case study based on CSX Corporation's intermodal rail-truck network in the United States as a realistic size problem instance in order to evaluate its performance and gain managerial insight.

The remainder of this paper is organized as follows. Chapter 2 is dedicated to a review of relevant literature. In Chapter 3, we provide a description of our proposed disruption risk mitigation methodology and present a realistic case study. In Chapter 4, the mathematical modeling framework i.e. the bi-objective optimization model is defined and parameter estimation techniques are elaborated. Chapter 5 summarizes the results of computational experiments performed by solving the optimization program for the aforementioned case study. In Chapter 6, we delve into the details of the predictive analytics that are at the heart of our proposed disruption risk mitigation methodology. Ultimately, we outline our conclusions, contributions and suggestions for future research in Chapter 7.

Chapter 2

Literature review

In order to provide a comprehensive exposition of the research done in this field and to obtain a better understanding of where this study fits in the bigger picture of the existing literature, we elaborate the pertinent literature under the following three areas of study: hazmat risk assessment, rail-truck intermodal transportation of hazmat and disruption management.

2.1 Hazmat risk assessment methodologies

Despite all the efforts of transportation companies and government agencies to reduce the risks associated with hazardous material transportation, the possibility of highly damaging accidents catalyzing the release of dangerous substances still lingers (Verma & Verter, 2013). Consequently, many researchers have tried to capture different aspects of the aforementioned risk through dif-

ferent methodologies. A review of popular risk assessment methodologies and the seminal works introducing them will be provided in this section.

2.1.1 Expected consequence

The most prevalent definition of risk is described as the product of the consequences of an harmful event and the probability of such an event happening. This measure is commonly referred to as "traditional risk" in the hazmat transportation domain. Erkut and Verter (1998) approach this risk assessment metric in the transportation setting by calculating, for every arc in a path, the product of the likely consequences of an accident and the arc's accident probability, and considering the path's traditional risk to be equal to the sum of these products.

This methodology has been used in studies such as Alp (1995) and Erkut and Verter (1995) in the highway domain and was afterwards adapted to the assessment of risk in the railroad domain in the works of Bubbico et al. (2004) and Verma (2011). This risk measure has some advantages since it incorporates both the probability of an actual accident event as well as the consequences of the incident. However, the pertinent data required to implement this method is not available and/or accessible in many cases and this consideration has resulted in the formulation of other measures of risk.

2.1.2 Population exposure

Scholars have defined a new risk measure, based on one extreme of the traditional expected consequence risk spectrum, which only concerns itself with the total population number exposed to hazmat transportation risk and called it population exposure. This approach might be more suitable when the hazmat type being transported entails an exposure risk for the surrounding population, for instance radiation from nuclear waste or other radioactive material. This measure was initially developed in the highway domain in studies by Batta and Chiu (1988) and ReVelle et al. (1991) and was later adjusted based on the dynamics of train transportation by Verma and Verter (2007) to be used in the railroad domain.

2.1.3 Incidence probability

On the other side of this consequence-probability continuum is the incident probability measure which concerns itself with minimizing the likelihood of a transportation incident. This measure is quite useful when the transported hazmat creates a small radius of danger or when the decision maker is very intolerant of hazmat release incidents and wants to minimize the probability of such events. This model of risk assessment has been adopted by Saccomanno and Chan (1985) for the highway domain and was later adapted by Bagheri

et al. (2011) to take into account the intricacies of the railroad domain and to be used for minimizing the risks of hazmat train accidents.

2.1.4 Risk-averse methods

Since the traditional risk measure doesn't incorporate the risk preferences of decision makers and the negative public perception towards hazmat transportation, efforts were made to capture this risk-aversion. This led to the introduction of the perceived risk model which modeled risk aversion through the use of a risk preference parameter (Abkowitz et al., 1992). The challenges of accurately understanding and quantifying the risk preference factor motivated Erkut and Ingolfsson (2000) to develop three catastrophe avoidance models namely, mean-variance, maximum risk and disutility for the highway domain. In an effort to extend this work to the railroad domain, Jabbarzadeh et al. (2019) developed a risk measure that mixes expected risk and variability in risk through the use of absolute deviation instead of variance.

Kang et al. (2014a, 2014b) argue that there are risk confidence level intervals in which none of the above-mentioned methods can guarantee an optimally safe route for hazmat freight and propose the value-at-risk (VaR) method which captures the preferences of decision makers and generates dissimilar routes for hazmat freight in the trucking domain. Subsequently, Hos-

seini and Verma (2017) adapted the VaR based methodology for the problem of planning rail hazmat shipment routes. However, the VaR model has not been widely accepted since it is not a consistent risk measure and its performance might be poor in some problem instances (Toumazis & Kwon, 2013).

The deficiencies of the VaR method and the conditional value-at-risk (CVaR) model's ability to generate risk-averse and flexible hazmat shipment routes and its focus on avoiding extremely consequential events inspired Toumazis et al. (2013) to adapt CVaR model for the highway domain, and Toumazis and Kwon (2016) developed this methodology further. The same measure was used in Faghih-Roohi et al. (2016) as the main objective in the dynamic optimization of routing and scheduling of highway hazmat shipments. Subsequently, Hosseini and Verma (2018) developed a CVaR risk assessment methodology for hazardous material rail transportation. Finally, Su et al. (2019) propose the use of spectral risk measures for the problem of hazmat shipment risk-averse routing with the goal of obtaining more desirable solutions in those instances that CVaR or other popular risk measures fail to provide the safest paths.

2.1.5 Environmental risk

It is worthy to note that the main focus of the aforementioned studies was to model the risk of hazmat transportation for the exposed population. The im-

pact of hazardous material release during road transportation on a number of vulnerable environmental elements was considered in Martıénez-Alegrıéa et al. (2003). Cordeiro et al. (2016) created a framework for the process of assessing the environmental risks of hazmat road transportation; while, Machado et al. (2018) developed a multi-criteria spatial analysis tool and concluded that geology, drainage density and soil type are key factors in determining the vulnerability of highway segments to hazardous material spills.

In an effort to account for the environmental risks of moving hazmat on railroad networks, Saat et al. (2014) proposed a quantitative methodology that calculated the cost of population evacuation and train delay as well as soil and groundwater cleanup, and multiplied them by accident release rates for different chemicals to obtain an estimate of annual risk costs.

2.2 Rail-truck intermodal transportation of hazmat

Hazardous materials transportation literature is very expansive and a large number of studies have been done in this area. Erkut et al. (2007) classify the research in this field into four domains: risk assessment, routing, facility location and routing and network design. We have already provided an overview of the seminal works in the risk assessment area and now we will turn our attention to the routing of hazmat and more specifically to the routing without

scheduling problems which are the most relevant to our present study.

Since a very large body of work exists in the literature of routing problems for road networks, and in the interest of brevity, we invite the reader to refer to Holeczek (2019) for a recent comprehensive and structured review of research in the field of hazardous material truck transportation problems.

In the railroad transportation of hazmat domain, one of the first studies was done by Glickman (1983) who evaluated the effects of rerouting shipments through more sparsely populated areas and concluded that hazmat transportation risk can be significantly reduced by this method. This idea is further investigated in Glickman et al. (2007) and the benefits of evaluating the risk-cost tradeoff in routing decisions are emphasized. Furthermore, a tactical model of railroad hazmat shipment planning and routing was developed by Verma (2009) who incorporated an expected risk calculation method based on the sequence of events ending in hazmat release from multiple tank cars. In another study, Verma et al. (2011) used the population exposure risk assessment framework presented in Verma and Verter (2007) for measuring risk and solved the routing problem through a meta heuristic solution methodology. In a recent study, Bornay et al. (2020) incorporated spatial risk along both network links and yards in their hazmat shipment routing problem formulation and discussed the effects of commodity flow bifurcation on risk-cost tradeoffs.

We now turn our attention to the rail-truck intermodal transportation mode that utilizes the combination of road and rail and is the focus of our current study. Rail-truck intermodal transportation of regular freight has been a well-studied area of research in the preceding years and the literature of this field is rich (Bontekoning et al., 2004; SteadieSeifi et al., 2014). However, comparatively fewer endeavors have tried to tackle the rail-truck intermodal transportation of hazardous materials. Motivated by the possibility of a potential hazmat transport risk reduction, Mazzarotta (2002) and Bubbico et al. (2006) concluded through transport risk analysis that a significant reduction in risk is possible by changing the mode of hazmat transportation from trucking to rail-truck intermodal.

In order to evaluate the trade-offs and benefits of hazmat rail-truck intermodal transportation, Verma and Verter (2008) presented and analyzed an expository Canadian case study. Using the knowledge gained in their previous study, Verma and Verter (2010) approached the modeling of a rail-truck intermodal transportation system by introducing an analytical framework for planning shipments of hazmat and regular freight in a rail-truck intermodal network in which shippers and receivers can access a sole pair of terminals through drayage. This work was extended to the most realistic case of this intermodal system i.e. shippers/receivers having access to multiple terminals in Verma et al. (2012).

Assadipour et al. (2015) incorporated congestion and equipment capacity at intermodal terminals in their model formulation for hazmat and regular freight transportation in a rail-truck intermodal terminal. They presented a bi-objective nonlinear mixed-integer program and provided the solution for a realistic size problem instance via a multi-objective genetic algorithm. In another study, Assadipour et al. (2016) developed a bi-level, bi-objective model to regulate the movement of hazmat shipments in a rail-truck intermodal network in which the government imposes tolls to discourage the use of certain intermodal terminals.

In similar studies in the facility location and routing domain, Xie et al. (2012) develop a new bi-objective location and routing model to find the optimal location of intermodal terminals and optimal transportation routes for hazmat shipments in a multimodal network. Finally, Ghaderi and Burdett (2019) formulate the location routing problem of hazmat transportation in an intermodal network as a two-stage stochastic program and solve it via a number of algorithms, namely Maximum Likelihood Sampling, Sample Average Approximation, and a mixture of the two to compare their performance. Their model also considers the possibility of disruptions at transfer yards in an effort to improve the transportation network's reliability.

2.3 Disruption mitigation and management

Considering the importance of smooth transportation operations to the ever-growing and fast-paced modern economies and the dire consequences of a supply chain disruption on them, the significance of creating reliable transportation networks that can absorb or recover from potential disruption events cannot be ignored. In order to consider and plan for possible disruptions in transportation networks, researchers have introduced and studied concepts like redundancy, resilience, reliability, flexibility and vulnerability and tried to utilize them in assessing the impact of disruptions and the quality of transportation networks. An overview of these concepts can be found in Faturechi and Miller-Hooks (2015). Furthermore, Gu et al. (2020) review the similarities and differences of the concepts of reliability, resilience and vulnerability by analyzing relevant studies, and provide a comparison of their performance in assessing transportation networks through illustrative numerical examples.

Another disruption risk management approach that is more closely linked to the one we have adopted in this study concerns itself with the removal of individual nodes or links from the network and the consequent undesirable impact on transportation operations. In other words, a 100% functional capacity reduction in a single network component is considered and the impact on the network performance metrics is assessed by comparing the post-disruption re-

sults with the performance of the network in normal operating conditions. This approach provides some knowledge about the relative importance of a specific network element compared with all the other elements in that network. It is worthy to note that the network element's capacity reduction may not be directly associated with a real-world disruptive event, and is only incorporated as a disruption scenario. What follows is a survey of research done in the disruption management area divided by transportation mode.

2.3.1 Road networks

Initial research in the area of disruption modeling was done by Asakura (1999) who considered capacity reduction as a result of deteriorated roads and provided a definition for travel time reliability as the ratio of travel times in degraded state to the travel times in normal operating conditions. Nicholson and Du (1997) developed a mathematical model for a degradable transportation system based on traffic and supply/demand equilibrium to strategically evaluate the socio-economic impacts of network component degradation. A. Chen et al. (2002) presented capacity reliability as a novel evaluation criterion for assessing degradable road network performance and propose a framework based on network equilibrium, Monte Carlo methods and reliability analysis.

The aforementioned studies focused on quantifying the negative effects of

a capacity reduction in network components. Since then numerous studies have considered different disruption events and infrastructure criticality metrics in road networks through the lens of different objectives. We invite the reader to refer to Jenelius et al. (2006), Sohn (2006), Scott et al. (2006) and Sullivan et al. (2010) for some examples of relevant studies. Sullivan et al. (2009) categorize these studies by the goal they are pursuing, whether it is to minimize a network's vulnerability to failure as a result of disruption, or to maximize the network's potential to recover from or cope with a disruption, or its resistance to potential disruptions. They also make a distinction between degradation which refers to a minor reduction in capacity and disruption which implies major reductions in capacity or the complete closure of a link/node.

In an insightful study, Mattsson and Jenelius (2015) discuss the research on resilience and vulnerability of transportation systems and specify that research on vulnerability can be divided into studies based on topological properties of transport networks and studies that incorporate the supply and demand side to more comprehensively examine the impacts of disruption, while resilience refers to the system's ability to recover or maintain functionality following a disruption event. In the interest of brevity, we end the review of research in this area by inviting the reader to refer to Jafino et al. (2020) for a conceptual and empirical comparison of seventeen transport network criticality metrics extracted from the numerous studies done in this area.

2.3.2 Railroads

Although both passenger and freight flow through the network will be affected by a potential disruption, most of the works in railroad disruption management have been in the area of passenger transportation. We invite the reader to refer to Veelenturf et al. (2016) and Zhu and Goverde (2019) for relevant studies. In the freight transportation domain, one of the initial efforts to examine the impact of disruption on railroad networks was done by Peterson and Church (2008) who developed a framework to examine how the loss of one or more bridges or tunnels can affect train operations.

A developing and active research area in railway systems disruption/disturbance management is the real-time railway rescheduling which is discussed in the study of Cacchiani et al. (2014) and they provide an overview of recovery algorithms and models for disruption management through this method. Sato and Fukumura (2012) approach the management of daily railway disruptions in Japan by evaluating the strategy of freight train locomotive reassignment and rescheduling. In a more recent study, Altazin et al. (2020) investigate real-time rescheduling decisions and present the results of implementing their methodology in dense real life railway systems.

Bababeik et al. (2017) use bi-level models to assess the vulnerability of

rail networks through the identification of links which if disrupted will impose the most transportation cost/delay, and additionally to capture and minimize the costs of rerouting and rescheduling of trains on the functioning sections of the network after the critical links become dysfunctional due to disruption. A new measure of link criticality called link exposure is introduced in Bababeik et al. (2018) and a bi-objective model is proposed to optimally locate relief trains along the more critical links in the rail network to increase its resilience towards disruptions. Jabbarzadeh et al. (2019) assess the effect of random disruptions on hazmat rail transportation and propose a novel risk measure as well as a bi-objective two-stage stochastic mathematical model to optimize hazmat shipment planning which incorporates the possibility of random disruptions.

Using the network element removal approach, Khaled et al. (2015) study train design and routing and try to minimize total cost of operations after a potential disruptive event that makes network infrastructure unavailable. They presented a linear mixed-integer program and provided its solution for a case study of a US based railroad operator by proposing an iterative heuristic algorithm. Since they assumed that if a link is disrupted, it becomes unavailable, the sole possible recovery strategy in this case would be to reroute shipments on undisrupted links of the network. Azad et al. (2016) extended their work by incorporating a few service leg repair scenarios, plus the possibility of re-sending shipments from their origin, as well as allowing for the use of third

party transportation following a disruption. Their aim was to make the model useful both for single link disruption events, and also in case multiple network links are disrupted.

Finally, Fikar et al. (2016) assess the effects of rail closures on the local industries through a decision support system that simulates passenger and freight flow on a rail network; subsequently, calculating delays due to link disruption and rerouting of traffic with the aim of identifying critical links and assessing the impact of said disruption in their case study which was based on a major Alpine corridor. While extending the analysis of network element criticality from single-commodity problems to multi-commodity networks, Whitman et al. (2017) propose a three-stage method based on multi-criteria decision analysis and multi-commodity flow optimization problem to identify the most important links with respect to distinct commodity categories moved on the Swedish railway system.

2.3.3 Rail-truck intermodal networks

In an effort to address and mitigate the effects of potential disruptive events in intermodal transportation networks, Huang et al. (2011) proposed a decision method that rerouted shipment flows if delay forecast for a link was greater than a pre-specified threshold. Ishfaq (2012) suggest that the use of two-

connected networks formed by multiple modes of transportation which provide each origin-destination pair with at least two edge-disjoint paths can contribute to network resilience against disruptions.

A stochastic mixed-integer mathematical model that minimizes unsatisfied demand in the event of a disruption was developed by L. Chen and Miller-Hooks (2012) who also defined and proposed a quantitative measure of intermodal freight network resilience. Miller-Hooks et al. (2012) further developed the previous study and this time tried to maximize intermodal transportation network's resiliency by including the possibility of taking preparedness and recovery actions within the confines of a given budget. They formulated a stochastic optimization program with the objective of maximizing freight flow in the network under disruption scenarios. Both of the previous works' models were applied to small-scale networks due to computational complexity.

Uddin and Huynh (2016) contributed to the field by developing a stochastic mixed-integer model to tackle the problem of determining optimal routes for freight shipments in a rail-truck intermodal network under disruption. They used the sample average approximation method to solve the model on two example networks. In a similar study, Uddin and Huynh (2019) developed a framework for finding the optimal routes for the transportation of multi-commodity freight in an intermodal network, while assuming a lower capacity

for network links and nodes. Their goal is to obtain a desired network reliability level by analytically determining the level of capacity reduction that should be considered in the planning phase. Most recently, Ke (2020) incorporated the possibility of random disruptions at intermodal terminals by developing a robust optimization model for hazmat shipment planning with the goal of minimizing mean and variability of risk in a rail-truck transportation network.

In one of the few studies in the literature that used the one-at-a-time arc/node elimination strategy in intermodal networks, Burgholzer et al. (2013) used real-life data to micro simulate traffic and measure delay time due to disruptions in intermodal transportation networks. The delay impact of partial (50%) or complete (100%) disruptions on specific links was then used to rank links in terms of how critical they are for the network and to measure criticality of the network as a whole.

Review of pertinent literature illustrates the fact that most of the research done in the area of disruption risk management in rail-truck intermodal networks focuses on regular freight and minimizing disruption impacts through rerouting. To the best of our knowledge, no previous study has tackled the problem of developing disruption risk mitigation strategies based on the identification of critical infrastructure via bi-objective optimization and machine learning in multiclass hazmat rail-truck intermodal transportation networks.

The risks associated with the transportation of hazmat as well as the total cost of operations are two conflicting objectives that compel the decision makers to adopt a customized approach to this problem such as the one presented in this study. It is worthy to note that our usage of a supervised learning technique called classification for predictive analysis is unique in this context.

We have made an effort to fill the gap in the literature by proposing a methodology based on the combination of a bi-objective tactical shipment planning/routing optimization model and machine learning techniques that enables us to more efficiently identify the most critical infrastructure in the network i.e. the train service legs and intermodal terminals, the disruption of which has the highest negative impact on the total transportation cost and risk. The ultimate goal of this method is to equip the company's managers with the knowledge of the critical network elements, so that they can plan mitigation strategies in advance of a disruption event, and optimally assign limited disruption risk mitigation resources to the most critical infrastructure.

Chapter 3

Proposed methodology and case study

In this chapter, the aim is to describe our proposed methodology in more detail and discuss how it can be used in normal operating conditions of the network i.e. pre-disruption period as well as in case of an actual infrastructure disruption event i.e. post-disruption period. In the pre-disruption/planning period, the transportation company can use the mathematical model to optimally plan the movement of both regular and hazmat freight along the network, and the predictive classification model can be used as a useful tool in identifying the critical train service legs and intermodal terminals, so that mitigation strategies can be formulated and implemented to diminish the negative impacts of a potential disruption. In the post-disruption period, disruption events can be incorporated in the parameters of the model to obtain the optimal shipment rerouting solution.

Moreover, we present a novel case study in Section 3.2 that is based on the rail-truck intermodal transportation network of CSX Corporation in the US to illustrate the process of implementing this methodology in more detail.

3.1 Disruption risk mitigation methodology

This section is dedicated to the description of how our proposed disruption risk management methodology can aid companies offering rail-truck intermodal transportation services in planning for disruption mitigation and recovery strategies. Figure 1 illustrates a flowchart which summarizes the steps for implementing the proposed methodology. In summary, the ultimate goal of the method is to identify the critical train service legs and intermodal terminals via a combination of mathematical optimization and machine learning techniques in order to equip the transportation company's decision makers with the necessary knowledge required to optimally assign disruption mitigation resources. This goal can be achieved through the process outlined in more detail below.

In the first step, we need the input data for the tactical bi-objective routing optimization model (see Section 4.1 for further details) which comes in the form of transportation demand. Having obtained this demand data, we move on to the second step in which we solve the bi-objective shipment

planning optimization model to procure the optimal routing plan and number of trains needed. This helps us in calculating the total cost and total risk arising from the transportation of freight in the normal operating condition of the network which becomes the benchmark for measuring the negative impacts of disruption on the aforementioned objective function values.

In the third step, we need to decide whether the classification model developed in previous iterations of the cycle needs to be updated. Depending on the decision-maker's criteria which can include requiring an update after a certain number of transportation planning periods or in case of a significant change in demand volumes etc., we will decide whether to go through the process of updating the classification model or not. In the first few iterations of the cycle, we need to update the classification model every single iteration since one transportation period does not provide the supervised learning model with enough data points to train a robust model.

Assuming that the classification model needs to be updated, the next step involves solving the aforementioned bi-objective optimization model for as many times as there are service legs and terminals in the network each time incorporating the disruption of a single service leg or a single terminal in the parameters of the model. This helps us calculate the increase in total cost and total risk of transportation in the network due to a disruption in a service leg or

terminal compared to the benchmark which is the normal operating condition of the network. The fifth step is to obtain the disruption impact categories into which we intend to classify the infrastructure. This task is performed via a clustering algorithm that will aid us in finding the best possible categorization of the service legs and terminals.

The sixth step includes the extraction of feature data to be used alongside the labels obtained in the clustering step. These are the prerequisites needed to develop a classification model that predicts the disruption impact category (class) that each service leg or terminal belongs to based on a set of input features. Now we can utilize the trained classification model to classify the infrastructure in the current or next planning period.

If at the third step, we conclude that the classification model does not require an update, we can skip steps four to six and go straight to the seventh step which entails using the supervised learning model trained on the previous data to classify the infrastructure for the current transportation period. This is considerably more computationally efficient compared with the other method which entails obtaining actual post-disruption negative impacts through solving the routing optimization model for every single disruption scenario.

The final step involves another decision making task in which the man-

agers of the company devise mitigation strategies and decide which strategy should be implemented on which class of service leg or terminal, considering the company's budget and resource constraints. The idea is to optimally assign limited disruption risk mitigation resources to the most critical infrastructure so that the negative impacts of a potential disruption event are minimized.

A possible disruption risk mitigation strategy is to increase redundancy in the transportation network. For train service legs, this translates into building additional train tracks or renting other railroad operators' tracks in order to create additional paths and thus provide more options for shipment routing in case of a disruption. It should be noted that since the planning period considered in this study is relatively short and building new train tracks requires expensive long-term investment from the transportation company, renting the competitors train tracks appears to be more financially prudent. As for the intermodal terminals, building or renting additional cranes will create a backup plan in case of a random disruption, while specialized repair crews can also be deployed to respond quickly and restore the equipment to normal operating condition.

Once the mitigation strategies have been implemented, the process ends for the current transportation period and we move on to the next transportation period and repeat the process at the demand data procurement stage.

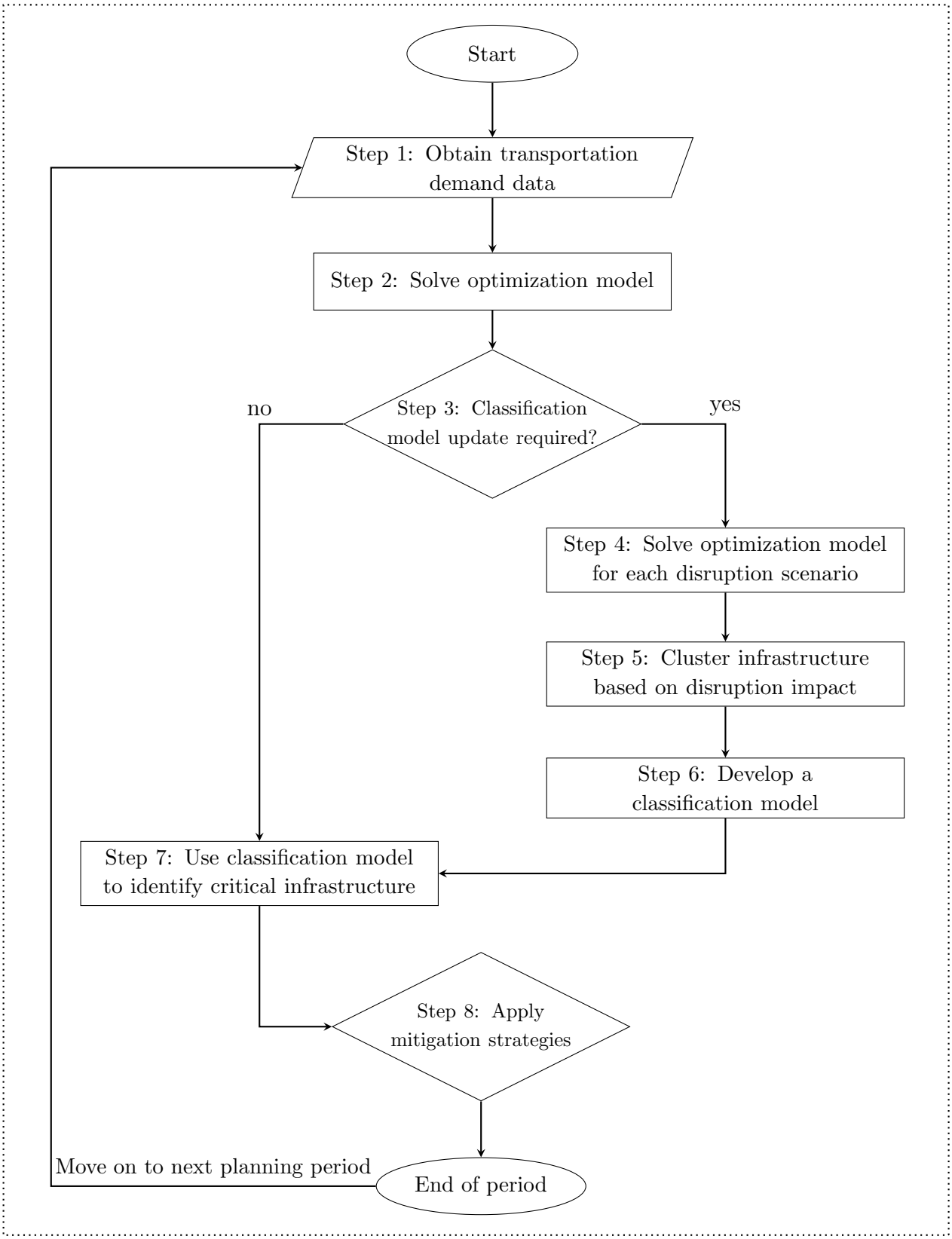

Figure 1: Flowchart of the proposed methodology

3.2 Case study setting

In order to be able to implement the proposed disruption risk mitigation methodology and evaluate its performance, we have created a novel case study to be used as a realistic problem instance based on CSX Corporation's intermodal rail-truck transportation network in the north-east, south-east and mid-west regions of the United States. The features of the aforementioned example network will be further explored in this section in order to illustrate the nuances and complexities of a realistic rail-truck intermodal transportation service chain.

Figure 2 depicts a map of our case study network which has been recreated using the ArcGIS software (ESRI, 2020) with white points that encompass a train symbol representing 16 intermodal terminals belonging to CSX Corporation which are access points for 24 shipper/receiver cities represented by red points and selected based on their proximity to at least two of the available intermodal terminals. Each shipper/receiver city has been selected such that it has access to at least two intermodal terminals in case one of them is disrupted and loses its functionality. In that case, customer demand can still be met using the other terminals, avoiding problem infeasibility. Finally, the black lines signify the rail tracks owned by CSX Corporation.

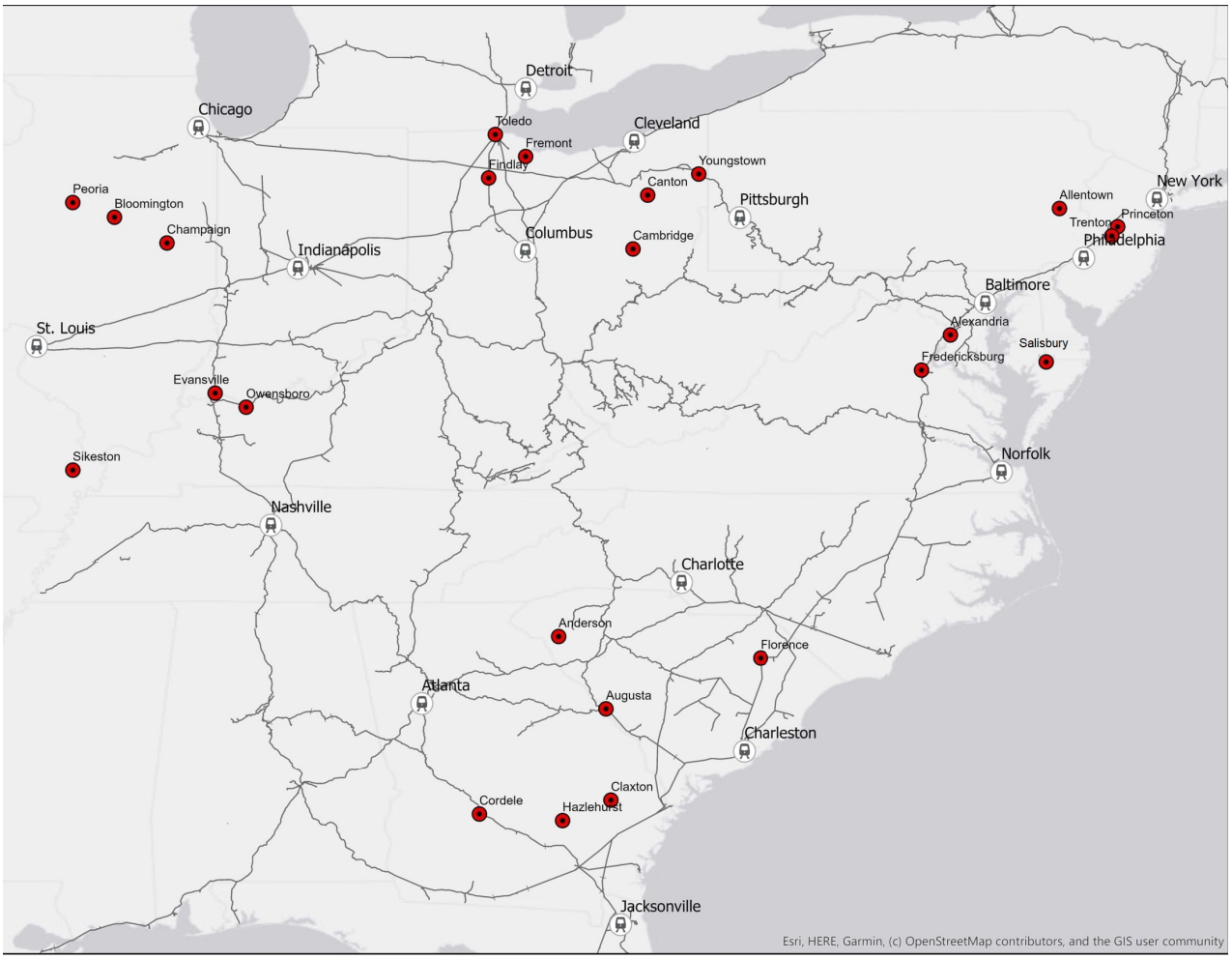

Figure 2: Map of the CSX intermodal network case study

As can be seen in Figure 2, the terminals and shipper/receivers in the network can be divided into four geographical regions, each of which consists of four intermodal terminals and six supply/demand nodes. The network is designed in such a way that each intermodal terminal serves three or four shippers/receivers and each shipper/receiver has access to at least two intermodal terminals. In total, there are 27 train service legs i.e. train tracks between two

consecutive train yards (terminals), and 32 types of intermodal train services, each with its own unique itinerary and intermediate stops, are using those service legs to operate in the network.

Demand data used in this study for the base-case problem instance is hypothetical and based on the shipper/receiver's city population; and in the additional problem instances, the demands have been randomly varied to account for the fluctuating nature of demand for regular and hazmat freight transportation services from one transportation period to another. It should be noted that in our case study no demand will be generated between cities that are in the same geographical region and/or in close proximity of each other since transportation demand in those cases will most likely be met using the highway infrastructure as opposed to a complete rail-truck intermodal chain. Respecting the above-mentioned conditions and pairing each shipper and receiver results in 432 supply and demand pairs i.e. traffic-classes. Each traffic-class will be assigned a delivery deadline and a transportation demand for regular/hazmat freight, the details of which will be further elaborated in the parameter estimation section.

Further details for estimating parameters such as transport risk for every link in the network along with all the other parameters will be further explained in Section 4.2.

Chapter 4

Modeling framework

In this chapter, we present a bi-objective mathematical formulation for the tactical hazmat/regular freight shipment planning and routing problem which also incorporates the possibility of disruption in one or more of the train service legs and/or intermodal terminals.

4.1 Mathematical formulation

Rail-truck intermodal transportation chains are typically comprised of the following links: (I) Inbound drayage i.e. transportation of freight from shipper to origin terminal; (II) Rail-haul i.e. transportation of freight from origin terminal to destination terminal; (III) Outbound drayage i.e. transportation of freight from the destination terminal to the location of the receiver. Demand of each customer (receiver) will be met by transportation of freight on the

path created by joining these three links. We use distinct flow variables for regular and hazmat freight to track their movement separately, since we need to incorporate the risk associated with hazmat cargo in addition to the cost attributes of both types of freight.

The mathematical notations used in the formulation of the model will be introduced below. It is wort noting that since this model has been inspired by the work of Verma et al. (2012), we have used similar notations whenever possible for convenience.

Notations

Sets

I	Set of shipper locations indexed by i
J	Set of receiver locations indexed by j
A	Set of origin intermodal terminals indexed by a
B	Set of destination intermodal terminals indexed by b
Z_{ij}	Set of shipper-receiver pairs (traffic-classes) indexed by z
P_{ia}	Set of arcs for inbound drayage indexed by p
R_{ab}	Set of rail routes between each intermodal terminal pair indexed by r
Q_{bj}	Set of arcs for outbound drayage indexed by q

K Set of hazmat classes indexed by k

V Set of intermodal train services indexed by v

S Set of service legs indexed by s

Parameters

C^p Cost of inbound drayage for a single hazmat container on arc p

$\bar{C}^p$ Cost of inbound drayage for a single regular container on arc p

C^r Cost of using rail route r to move a single hazmat container

$\bar{C}^r$ Cost of using rail route r to move a single regular container

C^q Cost of outbound drayage for a single hazmat container on arc q

$\bar{C}^q$ Cost of outbound drayage for a single regular container on arc q

FC^v Fixed cost incurred by using intermodal train service type v

PC_z Penalty cost per container per unit time of traffic class z

T^p Travel time of arc p for inbound drayage

T^r Travel time of rail route r

T^q Travel time of arc q for outbound drayage

DT_z Delivery deadline of traffic-class z

U^v Container loading capacity of intermodal train service of type v

G_s Equals 1 if service leg s is undisrupted; 0 otherwise

G_a Equals 1 if terminal a is undisrupted; 0 otherwise

G_b Equals 1 if terminal b is undisrupted; 0 otherwise

H_k^p Risk arising from moving a single hazmat container of type k on arc p

H_k^r Risk arising from moving a single hazmat container of type k using rail route r

H_k^q Risk arising from moving a single hazmat container of type k on arc q

D_{kz} Demand for containers of hazmat type k demanded in traffic-class z

$\bar{D}_z$ Demand for regular freight containers in traffic-class z

α_v^r Equals 1 if rail route r uses train service v; 0 otherwise

β_s^r Equals 1 if rail route r uses service leg s; 0 otherwise

M A large positive integer such that $M \geq \sum_{z \in Z_{ij}} (\sum_{k \in K} D_{kz} + \bar{D}_z)$

Variables

X_{kz}^p Number of hazmat containers of type k using arc p in traffic-class z

$\bar{X}_z^p$ Number of regular containers using arc p in traffic-class z

X_{kz}^r Number of hazmat containers of type k using rail route r in traffic-class z

$\bar{X}_z^r$ Number of regular containers using rail route r in traffic-class z

X_{kz}^q Number of hazmat containers of type k using arc q in traffic-class z

$\bar{X}_z^q$ Number of regular containers using arc q in traffic-class z

Y_{kz}^{prq} Proportion of hazmat type k freight demand of traffic-class z that is fulfilled using path prq

$\bar{Y}_z^{prq}$ Proportion of regular freight demand of traffic-class z that is fulfilled using path prq

N^v Number of intermodal train services of type v

Bi-objective Optimization Model

$$
\begin{aligned}
\text{minimize} \quad & \textbf{Cost: } \sum_{z\in Z_{ij}} \sum_{p\in P_{ia}} \left[\sum_{k\in K} \left(C^p X^p_{kz} \right) + \bar{C}^p \bar{X}^p_z \right] + \\
& \sum_{z\in Z_{ij}} \sum_{r\in R_{ab}} \left[\sum_{k\in K} \left(C^r X^r_{kz} \right) + \bar{C}^r \bar{X}^r_z \right] + \\
& \sum_{z\in Z_{ij}} \sum_{q\in Q_{bj}} \left[\sum_{k\in K} \left(C^q X^q_{kz} \right) + \bar{C}^q \bar{X}^q_z \right] + \\
& \sum_{v\in V} FC^v N^v \; + \sum_{z\in Z_{ij}} \sum_{p\in P_{ia}} \sum_{r\in R_{ab}} \sum_{q\in Q_{bj}} \\
& \underbrace{\left[PC_z \left(\left(T^p + T^r + T^q \right) - DT_z \right) \left(\bar{Y}^{prq}_z \bar{D}_z + \left(\sum_{k\in K} Y^{prq}_{kz} D_{kz} \right) \right) \right]}_{if \; \left(T^p + T^r + T^q \right) > DT_z} \\
& \textbf{Risk: } \sum_{z\in Z_{ij}} \sum_{p\in P_{ia}} \sum_{k\in K} \left[H^p_k \; X^p_{kz} \right] \; + \sum_{z\in Z_{ij}} \sum_{r\in R_{ab}} \sum_{k\in K} \left[H^r_k \; X^r_{kz} \right] + \\
& \sum_{z\in Z_{ij}} \sum_{q\in Q_{bj}} \sum_{k\in K} \left[H^q_k \; X^q_{kz} \right]
\end{aligned}
$$

subject to

$$\sum_{p\in P_{ia}} X^p_{kz} = \sum_{r\in R_{ab}} X^r_{kz} \qquad \forall a \in A, \;\; \forall z \in Z_{ij}, \;\; \forall k \in K \tag{1.a}$$

$$\sum_{p\in P_{ia}} \bar{X}^p_z = \sum_{r\in R_{ab}} \bar{X}^r_z \qquad \forall a \in A, \;\; \forall z \in Z_{ij} \tag{1.b}$$

$$\sum_{r\in R_{ab}} X^r_{kz} = \sum_{q\in Q_{bj}} X^q_{kz} \qquad \forall b \in B, \;\; \forall z \in Z_{ij}, \;\; \forall k \in K \tag{1.c}$$

$$\sum_{r\in R_{ab}} \bar{X}^r_z = \sum_{q\in Q_{bj}} \bar{X}^q_z \qquad \forall b \in B, \;\; \forall z \in Z_{ij} \tag{1.d}$$

$$\sum_{q\in Q_{bj}} X^q_{kz} = D_{kz} \qquad \forall z \in Z_{ij},\ \ \forall k \in K \tag{2.a}$$

$$\sum_{q\in Q_{bj}} \bar{X}^q_{z} = \bar{D}_{z} \qquad \forall z \in Z_{ij} \tag{2.b}$$

$$\sum_{z\in Z_{ij}} \sum_{r\in R_{ab}} \left[\Big(\sum_{k\in K} \alpha^r_v \beta^r_s \ X^r_{kz} \Big) \ + \Big(\alpha^r_v \beta^r_s \ \bar{X}^r_z \Big) \right] \leq U^v N^v \quad \forall s \in S,\ \ \forall v \in V \tag{3}$$

$$\sum_{z\in Z_{ij}} \sum_{r\in R_{ab}} \left[\Big(\sum_{k\in K} \beta^r_s X^r_{kz} \Big) \ + \Big(\beta^r_s \ \bar{X}^r_z \Big) \right] \leq \ MG_s \qquad \forall\ s \in S \tag{4}$$

$$\sum_{z\in Z_{ij}} \sum_{r\in R_{ab}} \Big(\sum_{k\in K} X^r_{kz} + \bar{X}^r_z \Big) \leq \ MG_a \qquad \forall a \in A \tag{5.a}$$

$$\sum_{z\in Z_{ij}} \sum_{r\in R_{ab}} \Big(\sum_{k\in K} X^r_{kz} + \bar{X}^r_z \Big) \leq \ MG^b \qquad \forall b \in B \tag{5.b}$$

$$\sum_{q\in Q_{bj}} \sum_{r\in R_{ab}} Y^{prq}_{kz} D_{kz} = \ X^p_{kz} \qquad \forall p \in P_{ia},\ \ \forall z \in Z_{ij},\ \ \forall k \in K \tag{6.a}$$

$$\sum_{q\in Q_{bj}} \sum_{r\in R_{ab}} \bar{Y}^{prq}_{z} \bar{D}_{z} = \ \bar{X}^p_z \qquad \forall p \in P_{ia},\ \ \forall z \in Z_{ij} \tag{6.b}$$

$$\sum_{p\in P_{ia}} \sum_{q\in Q_{bj}} Y^{prq}_{kz} D_{kz} = \ X^r_{kz} \qquad \forall r \in R_{ab},\ \ \forall z \in Z_{ij},\ \ \forall k \in K \tag{6.c}$$

$$\sum_{p\in P_{ia}} \sum_{q\in Q_{bj}} \bar{Y}^{prq}_{z} \bar{D}_{z} = \ \bar{X}^r_z \qquad \forall r \in R_{ab},\ \ \forall z \in Z_{ij} \tag{6.d}$$

$$\sum_{p\in P_{ia}} \sum_{r\in R_{ab}} Y^{prq}_{kz} D_{kz} = \ X^q_{kz} \qquad \forall q \in Q_{bj},\ \ \forall z \in Z_{ij},\ \ \forall k \in K \tag{6.e}$$

$$\sum_{p\in P_{ia}} \sum_{r\in R_{ab}} \bar{Y}^{prq}_{z} \bar{D}_{z} = \ \bar{X}^q_z \qquad \forall q \in Q_{bj},\ \ \forall z \in Z_{ij} \tag{6.f}$$

$$X^p_{kz} \geq 0,\ \ \bar{X}^p_z \geq 0 \qquad integer \qquad \forall p \in P_{ia},\ \ \forall z \in Z_{ij},\ \ \forall k \in K \tag{7.a}$$

$$X^r_{kz} \geq 0,\ \ \bar{X}^r_z \geq 0 \qquad integer \qquad \forall r \in R_{ab},\ \ \forall z \in Z_{ij}\ \ \forall k \in K \tag{7.b}$$

$$X^q_{kz} \geq 0, \;\; \bar{X}^q_z \geq 0 \qquad integer \qquad \forall q \in Q_{bj}, \;\; \forall z \in Z_{ij} \;\; \forall k \in K \tag{7.c}$$

$$N^v \geq 0 \qquad integer \qquad \forall v \in V \tag{7.d}$$

The mathematical model is a variant of the multicommodity flow problem which is NP-Hard to solve. In order to maintain the linearity of the model and to reduce the number of defined variables, we needed to preprocess the network which ultimately led to less computational complexity and 140400 continuous and 37664 integer variables in total. The model incorporates both cost and risk as objectives. The cost objective includes the cost of inbound drayage operations, rail-haul cost, the cost of outbound drayage, fixed cost of operating the train services in the network as well as the penalty cost incurred if the selected transportation path for a traffic-class has a travel time that exceeds its delivery deadline. The risk objective captures the transportation risk associated with moving hazmat cargo on the inbound drayage, rail-haul, and outbound drayage links.

Constraint (1) signifies the transshipment function of the intermodal terminals. Constraints (1.a) and (1.b) capture the transfer of hazmat and freight shipments respectively, from trucks coming through inbound drayage links to trains using rail routes to reach their destination terminals. Constraints (1.c) and (1.d) signify the transfer of hazmat and regular shipments from trains to

trucks that use outbound drayage links the deliver the freight to their intended receivers. Constraint (2) ensures the fulfillment of every receiver's demand for hazmat freight (2.a) and regular freight (2.b) using the trucks coming thorough outbound drayage links. Constraint (3) incorporates the capacities of the trains into the model and ensures that each intermodal train service type is assigned with the minimum number of trains that is required to transport the demanded containers on every service leg that it traverses. Constraint (4) ensures that if a train service leg is disrupted, no train route can use the disrupted service leg to transport freight. Constraints (5.a) and (5.b) ensure that if an intermodal terminal is disrupted, no loading or unloading of shipments can be performed on that disrupted terminal. Therefore, transport demand has to go through other terminals and rail routes. Constraint (6) calculates the value of the Y variables which signify the proportion of hazmat or regular demand that is fulfilled by transportation via each path (comprised of arcs p,r,q) in the network. Constraint (7) ensures the sign and integer requirements of the model.

4.2 Estimation of model parameters

A brief description of how we calculated each parameter used in the mathematical model is presented in the following subsections. Readily available

information was used to estimate these parameters. The adopted hazmat risk assessment methodology warranted a more detailed explanation because of its complexity and the need for a more clear distinction between our adopted approach and other approaches in the literature reviewed in Chapter 2.

4.2.1 Demands and capacities

Since demand for the transportation services of CSX Corporation between each shipper and receiver pair may vary week by week, we assigned hypothetical demand values to each pair based on the population of their respective cities. We assumed that a total of 20,000 intermodal containers need to be transported in the network, with each freight category i.e. hazmat and regular accounting for 10,000 containers. Data obtained from CSX Corporation shows that hazmat classes 2, 3 and 8 combined account for around 80 percent of all hazardous material cargo transported on the company's network (CSX, 2020a). Therefore, we limit the hazmat classes analyzed in this study to the aforementioned three, and assume that 30 percent of total hazardous material transported belongs to Class 2, 50 percent belongs to Class 3 and 20 percent belongs to Class 8. Finally, the capacity of intermodal trains is assumed to be 120 containers for all the trains operating in the network.

4.2.2 Travel times and deadlines

Average intermodal train speed was calculated to be 25.184 miles per hour using the historical data obtained from CSX Corporation's performance measures (CSX, 2020b). Therefore, the travel time for intermodal trains can be obtained by dividing the length of the arc by the aforementioned train speed. This average travel time also includes intermediate terminal dwell of the trains i.e. the total time in hours that trains spend at a given intermediate terminal. The maximum traveling speed for trucks differs by state in the US; nonetheless, we have assumed an average truck speed of 50 miles per hour, taking into account delays due to traffic congestion, traffic lights etc.

The lead time to satisfy demand for each traffic-class was calculated based on the shortest path available for that traffic-class plus a constant number of hours as a precautionary measure taken by the transportation company. In other words, delivery deadline was set equal to the the shortest possible travel time in hours for each traffic-class plus a buffer of 10 hours. For instance, if the shortest travel time between shipper A and receiver B was equal to 35 hours, the delivery deadline for this traffic-class would be 45 hours. The company has a contractual obligation to transport the intermodal containers before this pre-specified delivery deadline; otherwise, a penalty cost set to 40 dollars per container will be incurred per each hour of delay (Sarhadi et al., 2017).

4.2.3 Costs

The cost for drayage operations which is normally calculated based on the amount of time that the driver and the truck are engaged, was set to be 250 dollars per hour including the fuel cost; moreover, it is assumed that the cost of a container transfer at the intermodal terminal is 150 dollars and the operations for loading, unloading or transfer of an intermodal container take approximately one hour (Verma et al., 2012). Intermodal rail-haul cost was set to be 0.875 dollars per mile and the hourly fixed cost of operating an intermodal train was set to be 500 dollars per hour including the hourly compensation for the services of a driver, a brakeman and an engineer assumed to be 100 dollars each plus 200 dollars hourly rate for the engine (Verma et al., 2012).

4.2.4 Risk

Accidents leading to hazardous material release events can have many negative consequences for the population and property affected, as well as the surrounding environment. However, since the threat to human life is the most significant component and has received the most attention in relevant literature, this paper focuses solely on the hazmat incident consequence of human fatalities or serious injuries. According to Erkut and Verter (1995), we can

define the risk caused by transportation of a single shipment of hazmat type m via arc a for population center i as the product of individual risk and the number of people living in the said population center as can be seen in the following equation (from Erkut and Verter (1995)):

$$Risk_{aim} = IR_{aim} \times Q_i \tag{1}$$

where IR_{aim} is the risk to individuals in population center i and Q_i is the number of individuals residing at population center i. Risk to individuals in this case refers to the probability of death or serious injury.

If we divide the arc a into a set of homogeneous road segment denoted by s, IR_{aim} may be defined as the sum of individual risk arising from each road segment on arc a and can be obtained by the following formula (adopted from Zografos and Androutsopoulos (2004)):

$$IR_{aim} = \sum_{s} P_s(A) \times P_{sm}(R|A) \times P_m(I|R) \times P_{sim}(C|I) \tag{2}$$

where $P_s(A)$ is the probability of an accident that involves hazmat on road segment s, $P_{sm}(R|A)$ is hazmat release probability in case of an accident, $P_m(I|R)$ is the hazmat incident probability in case material m is released due to an accident, and $P_{sim}(C|I)$ is the probability of serious injury or death in case of a hazmat incident.

Since it is very hard and impractical to accurately estimate the impact

of a hazmat incident on individuals, many researchers (List et al., 1991) have simplified the previously mentioned formula by assuming that all individuals residing within a threshold distance λ from the hazmat incident are equally exposed to the risk of death or serious injury. This pragmatic approach leads to the following risk expression (from Zografos and Androutsopoulos (2004)) which has been adopted in this paper:

$$Risk_a^m = \sum_s p_s \times C_s^m \tag{3}$$

where $Risk_a^m$ is the total expected risk due to transportation of hazardous material m on arc a of the network, p_s is the probability of a release event on homogeneous road segment s of arc a, and C_s^m represents the consequences of a hazmat m release event such as the number of fatalities or serious injuries.

Since sufficient accident data might not be available for the probability of a hazmat incident on each individual arc in the network, we resort to a more aggregate measure which is the probability of an accident leading to a hazmat release incident over the whole network and use it as a substitute for the individual link's associated hazmat incident probability. Vaezi (2018) obtained the probability of hazmat release incident to be equal to 3.64×10^{-8} on the US rail network. This value signifies the probability of a hazmat release incident per each train mile traveled. Similarly, we have assumed the rate of 1.35×10^{-7} for drayage operations (FMCSA, 2001).

In order to obtain the threshold distance λ for each hazardous material studied in this research, impact areas were estimated using the ALOHA software (EPA, 2016). A representative chemical in ALOHA's database was chosen for hazmat classes 2, 3 and 8 and a scenario in which a full tank explodes and its chemical contents burn in a fireball is envisaged. The full list of assumptions and ALOHA input parameters for each hazmat class is provided in Table 1. The red zone which is a circle with radius of 0.32 miles for hazmat class 2, 0.28 miles for hazmat class 3 and 0.16 miles for hazmat class 8 signifies the area in which individuals are potentially exposed to death or serious injury.

Having obtained the aforementioned threshold distances, three buffers (one for each hazmat class) were created along each arc in the network using ArcGIS software (ESRI, 2020) and the number of individuals residing inside the impact area was calculated. This number multiplied by the corresponding incident probability is the hazmat risk associated with the transportation of a single hazmat container on that particular link in the network.

It is worth noting that a large number of hazmat risk assessment methodologies with the aim of estimating risks associated with transportation of hazardous materials on specific links in the network have been developed, as was elaborated in the literature review section, and the method adopted in this

study might not be the best one overall. However, since the focus of this study is on developing a methodology for disruption management, the risk assessment method adopted here should be adequate for our purposes.

Table 1: ALOHA input parameters

Hazmat Class	Class 2	Class 3	Class 8
Representative Chemical	Propane	Ethanol	Acetic Acid
Wind Speed (meters/sec)	10 (m/s)	10 (m/s)	10 (m/s)
Wind Measurement Height	3 meters	3 meters	3 meters
Ground Roughness	Urban or Forest	Urban or Forest	Urban or Forest
Cloud Cover	Partly Cloudy	Partly Cloudy	Partly Cloudy
Air Temperature	20°C	20°C	20°C
Stability Class	D	D	D
Inversion Height	No Inversion	No Inversion	No Inversion
Humidity	50%	50%	50%
Tank Type & Orientation	Horiz. cylinder	Horiz. cylinder	Horiz. cylinder
Diameter (feet)	10	9.7	8.09
Length (feet)	57	55	39
Volume (gallons)	33,500	30,500	15,000
State of Chemical	Liquid	Liquid	Liquid
Temperature within Tank	Ambient Temp	Ambient Temp	Ambient Temp
Liquid Level	100%	100%	100%
Type of Tank Failure	BLEVE	BLEVE	BLEVE
Potential Hazards	Thermal radiation from fireball	Thermal radiation from fireball	Thermal radiation from fireball
Tank Mass in Fireball	100%	100%	100%
Red Threat Zone	10 kW/(sq m)= potentially lethal within 60 sec	10 kW/(sq m)= potentially lethal within 60 sec	10 kW/(sq m)= potentially lethal within 60 sec

Chapter 5

Computational experiments

The focus of this chapter will be on providing an optimal solution to the mathematical optimization model developed and elaborated in the previous chapter. In the section called pre-disruption we will solve the model for normal operating circumstances of the network in which no service leg or terminal is dysfunctional. This can be accomplished either by removing constraints (4) and (5) from the model or adjusting the relevant parameters to the no disruption setting on any link or node. Subsequently, in the section called post-disruption, we will incorporate the disruption of a single service leg or a single terminal into the model by changing the parameter settings as required, and solve the model again until we have covered all the network elements one at a time.

Many techniques have been introduced in the literature for solving multi-

objective optimization models and one of the most widely used classical approaches is the weighted sum method which consists of attaching weights to every objective based on the decision-maker's preferences (Deb, 2001). As previously indicated, we define the managerial problem from the perspective of an intermodal transportation company interested in minimizing total cost of operations as well as the risk associated with the transportation of hazmat. We assume that the decision maker values both objectives equally, and thus assign identical weights to the cost and risk objectives in order to solve the model for normal operating circumstances, as well as each of the disruption scenarios. Nevertheless, we also report on the results and set of Pareto-optimal solutions obtained by attaching different weights to the cost and risk objectives in Section 5.1.1.

A necessary step that is required with the weighted sum approach is the normalization of the objectives. The cost objective which represents the total cost of operations is likely to be in millions of dollars, while the risk objective which represents the expected number of people that are exposed to the risk of death or serious injury may differ from the first objective by several orders of magnitude. In order to scale the two objective functions, Grodzevich and Romanko (2006) suggest we first solve the minimization problem of each objective function separately, obtaining the lower and upper bounds of the Pareto-optimal set called the Utopia (denoted by z_i^U) and Nadir (denoted by

z_i^N) points respectively, thus bounding the objective functions (denoted by $f_i(x)$) by (from Grodzevich and Romanko (2006)):

$$0 \leq \frac{f_i(x) - z_i^U}{z_i^N - z_i^U} \leq 1 \tag{4}$$

which brings both objective functions to the same order of magnitude.

All of the problem instances and the corresponding disruption scenarios analyzed in this study were solved using the Python API of Gurobi Optimizer version 9.0.2. (Gurobi Optimization, 2020). All the computation were performed on a laptop computer with INTEL Core i7-8550U CPU and 16 GB of RAM. The computational times for the different problem instances varied between roughly 2 and 20 minutes of CPU time.

5.1 Pre-disruption

For the purposes of this analysis, we define the *base-case* problem instance as the case representing the first planning period's demand data solved via assigning equal weights to both objectives. Having solved the base-case problem instance using the weighted sum approach with equal weights attached to both objectives after 5 minutes of CPU time, we summarize the obtained objective function values in Table 2. The specified transportation demand in the base-case problem instance can be met at the cost of \$62.6 million, and expected risk of 178.3 individuals. It is worth noting that a significant portion

of transportation cost stems from drayage operations. A small penalty cost has also been incurred which signifies the selection of longer paths to satisfy demand (compared with the shortest path for that traffic-class) in order to avoid exposing a significantly higher number of people to hazmat risks.

Table 2: Base-case solution

Cost			**Risk**	
Drayage	Rail-haul	Penalty Cost	Drayage	Rail-haul
48,610,400	13,992,786	20,675	103.268	75.103
Total Cost: 62,623,862			Total Risk: 178.372	

Table 3 provides more details about the 32 intermodal train service types operating in the network, with each single train having a capacity of 120 containers. For instance, the first row in the table represents the intermodal train service that starts its operations in Atlanta and ends them in Norfolk, with a single stop along the way in Charlotte. Only two trains are required to transport the assigned containers which will add a fixed rail-haul cost of $26,643 to the company's overall transport costs. As for the second intermodal train service which goes form the Baltimore terminal to the terminal in Chicago with a stop in Pittsburgh, a significantly higher number of trains i.e. 21 is needed to fulfill the assigned transportation demand which in turn incurs a much higher train fixed cost of $321,871. The relevant details about the other

train services in the network can be similarly interpreted.

It is evident from Table 3 that each of the train services operating between the intermodal terminals of Cleveland and Jacksonville, Detroit and Nashville, Detroit and Norfolk and St. Louis and Norfolk have only been assigned a single train. This underutilization might stem from the fact that demand in few traffic-classes is fulfilled via the paths that utilize these train services or that the demand in those traffic-classes is minimal. The company's decision makers might be interested in identifying the reasons behind this inefficiency and potentially add or remove some train services from the network.

It should be pointed out that the intermodal train services and their intermediate stops in our case study's network were designed with the objective of connecting every single intermodal terminal in each of our case study's geographical regions to every other intermodal terminal in all the other regions. This is an important and essential provision to ensure the connectivity of the network both in normal operating conditions and in case of disruption in one service leg or intermodal terminal. This consideration along with the fact that every shipper/receiver in our network is connected to at least two intermodal terminals makes it possible to fulfill the transportation contracts with the existing infrastructure. Therefore, even if a train service is underutilized in the base-case, it might play a crucial role in the case of a disruption event.

Table 3: Train service attributes

From	To	1st Stop	2nd Stop	Trains	Fixed Cost
Atlanta	***Norfolk***	Charlotte		2	26,643
Baltimore	***Chicago***	Pittsburgh		21	321,871
Charleston	***Detroit***	Charlotte	Columbus	12	240390
Chicago	***Baltimore***	Pittsburgh		21	321,871
Chicago	***Detroit***			6	36,928
Chicago	***Nashville***	Indianapolis		5	51,123
Chicago	***New York***	Cleveland		7	130,221
Cleveland	***Jacksonville***	Columbus	Atlanta	1	22,970
Columbus	***New York***	Cleveland		3	44,432
Columbus	***St. Louis***	Indianapolis		15	128,950
Detroit	***Pittsburgh***	Columbus	Cleveland	7	74,630
Detroit	***Chicago***			6	36,928
Detroit	***Nashville***			1	11,455
Detroit	***Charleston***	Columbus	Charlotte	13	260,423
Detroit	***Norfolk***	Columbus		1	16,836
Jacksonville	***Nashville***	Atlanta		8	94,980
Jacksonville	***Norfolk***	Charleston		8	99,428
Jacksonville	***Cleveland***	Atlanta	Columbus	1	22,970
Nashville	***Jacksonville***	Atlanta		11	130,598
Nashville	***Chicago***	Indianapolis		5	51,123
Nashville	***Detroit***			1	11,455
New York	***Columbus***	Cleveland		6	88,865
New York	***Norfolk***	Philadelphia	Baltimore	13	131,889
New York	***Chicago***	Cleveland		3	55,809
Norfolk	***St. Louis***	Indianapolis		1	20,409
Norfolk	***Detroit***	Columbus		1	16,836
Norfolk	***New York***	Baltimore	Philadelphia	13	131,889
Norfolk	***Jacksonville***	Charleston		8	99,428
Norfolk	***Atlanta***	Charlotte		2	26,643
Pittsburgh	***Detroit***	Cleveland	Columbus	8	85,292
St. Louis	***Columbus***	Indianapolis		13	111,757
St. Louis	***Norfolk***	Indianapolis		1	20,409

Since the focus of our study is to identify the critical network infrastructure owned by the transportation company i.e. the train tracks and intermodal terminals, and thus facilitating disruption risk mitigation planning, we try provide a better picture of the movement of freight in our network through the simple diagram in Figure 3 for the regular freight containers and Figure 4 for the hazmat freight containers. Figures 3 and 4 depict the rail-haul portion of the optimal solution found for the base-case problem instance. The nodes represent intermodal terminals and their size indicates the number of containers that are transferred from trucks to trains at this yard. The links represent train service legs and their width indicates the traffic density on that particular service leg.

It is evident from the diagrams that service leg and terminal utilization in the case of hazmat freight is more evenly distributed which is an ideal situation from a risk distribution perspective. However, when it comes to regular freight the terminals in Philadelphia, Baltimore, Cleveland, Detroit and Chicago are busier than the rest of terminals which indicates that a relatively larger number of shortest paths in the network utilize these terminals and towns with a higher population and consequently higher transportation demand are located close to these yards. Similarly, the Baltimore-Pittsburgh service leg has a higher traffic density which is due to its importance in connecting three geographical regions and its utilization in many of the shortest paths.

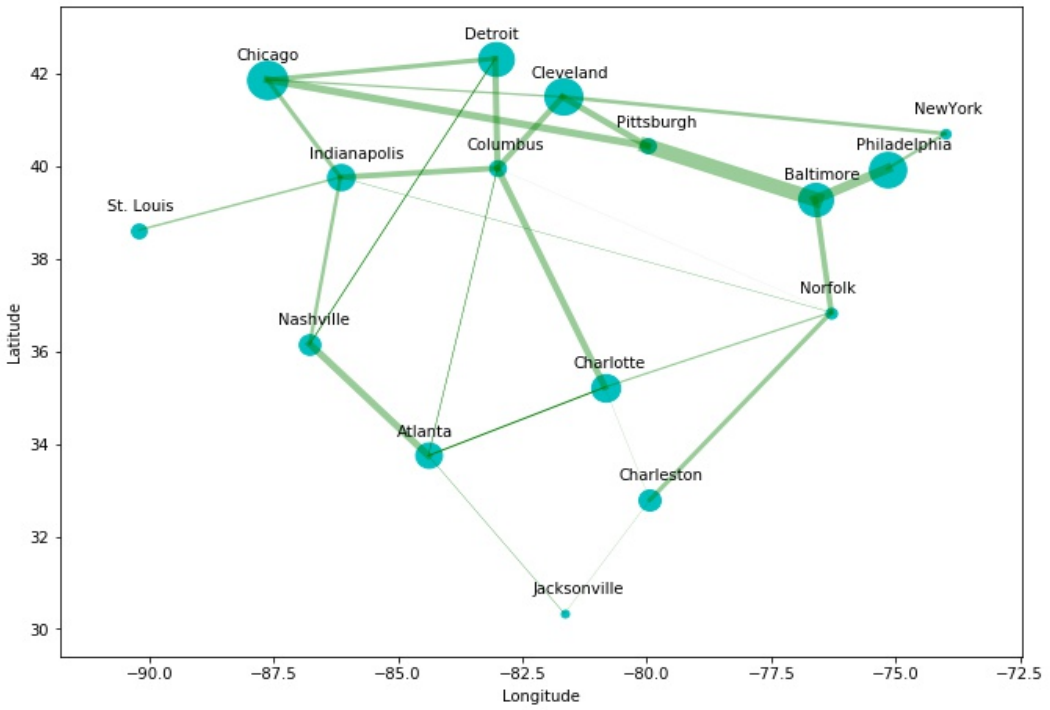

Figure 3: Service leg and terminal utilization (regular freight)

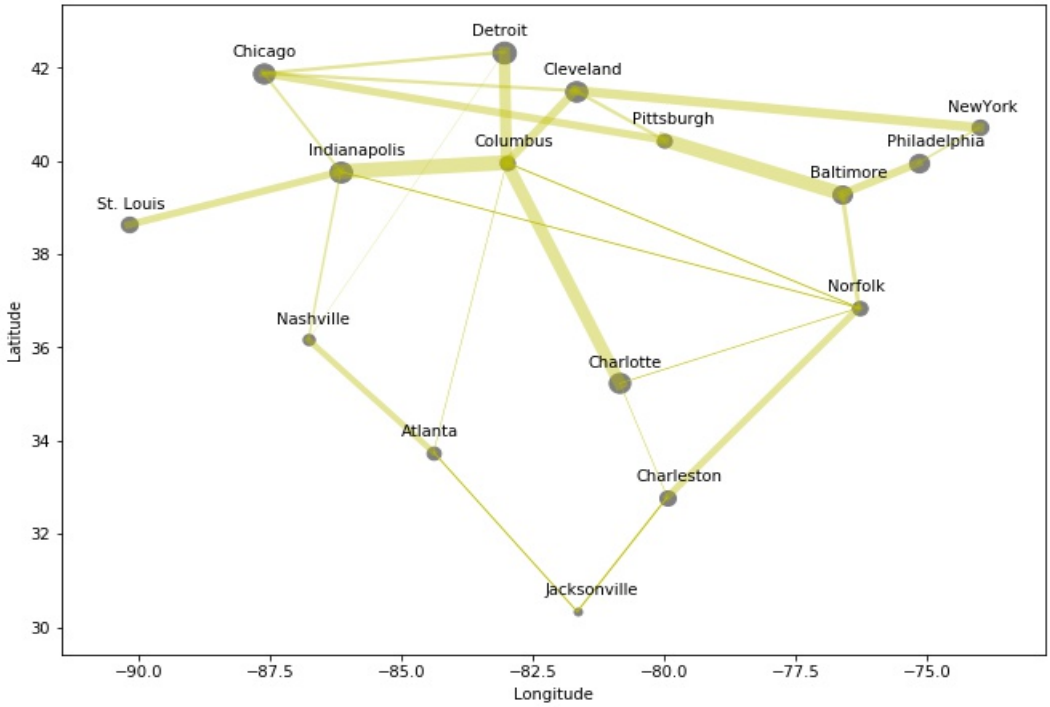

Figure 4: Service leg and terminal utilization (hazmat freight)

5.1.1 Cost-risk trade-off

This section is devoted to reporting and commenting on the impact of prioritizing one objective i.e. cost or risk over the other through varying the weights attached to the two objectives and solving the bi-objective routing optimization program for each case. Table 4 summarizes the solutions found in the form of total cost, total risk and total number of trains in the network and Figure 5 is a visual representation of the Pareto frontier. Every row in Table 4 and every point in Figure 5 signifies a non-inferior solution in the Pareto-optimal set with the min cost and min risk cases representing the two extremes and base case representing equal weights for both objectives.

We can see in Table 4 that the total cost in the min cost case is roughly \$61.7 million and the total risk is around 203 individuals, while the min risk solution incurs a total cost of \$65.1 million and exposes 171.5 to hazmat risks. This means that by spending an additional \$3.3 million dollars, it is possible to reduce the expected risk of death or serious injury by around 31.4 individuals. This might be of interest to hazmat regulators. Moreover, the min risk solution is 3.8% less risky and 4% more expensive than the base case, while the min cost solution is 13.8% more risky and 1.3% less expensive, with the increment in cost stemming from using longer but less risky paths for hazmat containers.

Table 4: Cost and risk trade-off numbers

Legend	Cost	Risk	No. of Trains
Min Cost	61,788,439	203.01	220
A: (cost, risk) = (0.9, 0.1)	61,833,594.	194.18	219
B: (cost, risk) = (0.8, 0.2)	61,906,414	189.98	220
C: (cost, risk) = (0.7, 0.3)	62,034,067	186.33	220
D: (cost, risk) = (0.6, 0.4)	62,292,888	182.03	224
Base Case	62,623,862	178.37	224
E: (cost, risk) = (0.4, 0.6)	62,859,998	176.58	226
F: (cost, risk) = (0.3, 0.7)	63,269,000	174.46	230
G: (cost, risk) = (0.2, 0.8)	63,692,907	173.12	236
H: (cost, risk) = (0.1, 0.9)	64,529,040	171.81	234
Min Risk	65,145,520	171.57	254

The number of trains required to fulfill transportation demand in the Min Cost case is 220, and the number of trains required in the Min Risk case is 254. This is an increase of 34 trains and means that prioritizing the risk objective function and utilizing less risky paths to deliver hazmat shipments may lead to them being moved on different paths compared with regular freight shipments, and thus more trains are utilized in the network. As we move from the side of the Pareto frontier that represents the Min Cost solution to the side that represents the Min Risk solution in Figure 5, the number of trains required in the network increases by around 15%.

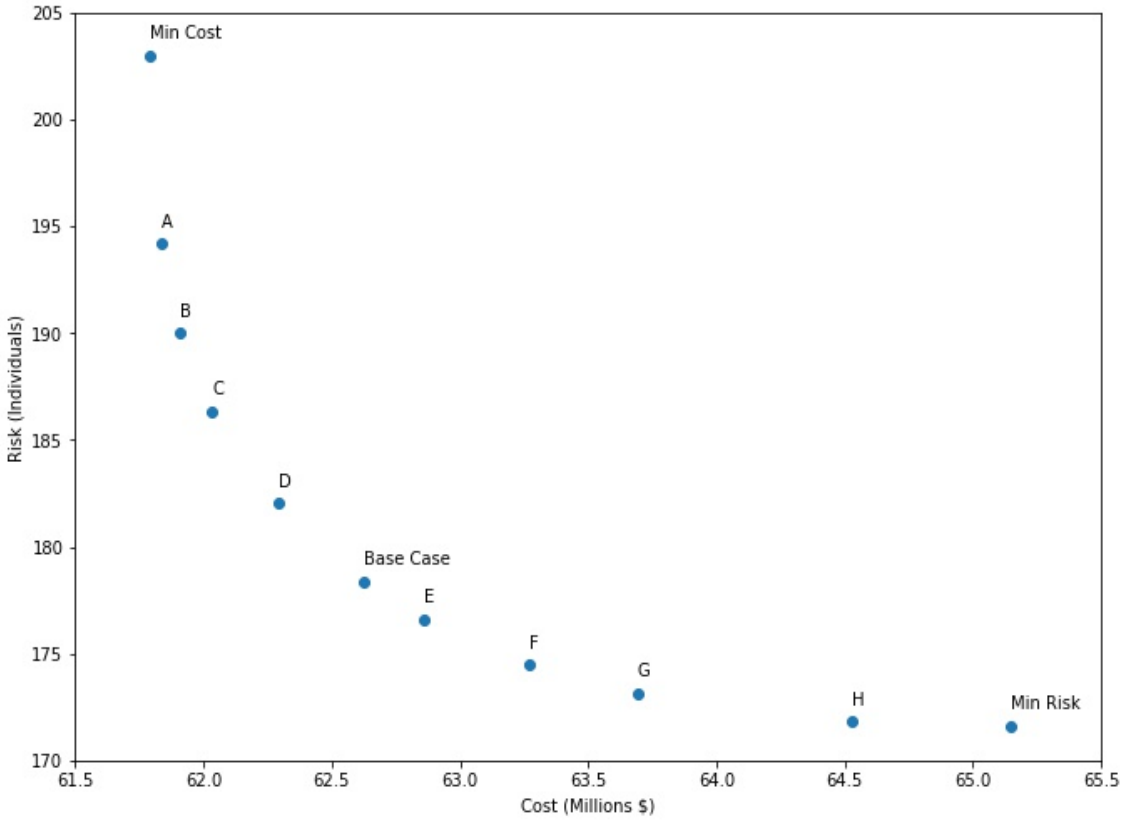

Figure 5: Cost - Risk trade-off

This shift in prioritization of objectives will inevitably lead to some path selection changes as well. To cite an example, we focus on the 20 Class III hazmat shipments that need to be transported from Allentown to Champaign. In the base-case, the containers are sent by truck from Allentown to New York and then continue the journey via train to Chicago, ultimately arriving by truck at their destination. However, in the Min Cost case, the selected origin intermodal terminal changes to Philadelphia, while in the Min Risk case, the selected destination intermodal terminal changes to Indianapolis.

5.2 Post-disruption

The loss of a part of the transportation network infrastructure such as one of the service legs or terminals due to random disruptions might potentially have an enormous impact on the efficiency of the network. In other words, the total cost and/or risk of fulfilling the customer demand for the transportation company may increase significantly since the shipments need to be rerouted through costlier and riskier paths. Therefore, it is in the transportation company's best interest to know about the magnitude of the potential impact of losing any of the company-owned infrastructure due to random disruption so that mitigation action can be taken prior to the actual disruption event to lessen the severity of consequences.

In order to assess the impact of the loss of a network element on the total network cost and risk, we incorporate the disruption of each individual service leg or terminal in the optimization model's parameters one by one, and then solve the model for each of these disruption scenarios. The results of this process have been summarized in Table 5 for service legs and in Table 6 for terminals. Columns 3 and 4 illustrate the network-wide cost and risk of transportation operations after the disruption, while columns 5 and 6 signify the difference between the aforementioned values and the total cost and risk in the base-case which acts as a benchmark of network performance.

Table 5: Post-disruption objective function values (service legs)

No.	Service Leg	Total Cost	Total Risk	Cost Increase	Risk Increase
1	Atlanta - Charlotte	62,812,865	183.593	189,003	5.221
2	Atlanta - Columbus	62,770,895	183.531	147,033	5.159
3	Atlanta - Jacksonville	62,894,529	184.142	270,666	5.770
4	Atlanta - Nashville	64,758,267	184.369	2,134,404	5.996
5	Baltimore - Norfolk	64,391,560	185.180	1,767,697	6.808
6	Baltimore - Philadelphia	64,500,143	187.312	1,876,280	8.940
7	Baltimore - Pittsburgh	64,910,534	189.863	2,286,671	11.491
8	Charleston - Charlotte	62,748,289	183.696	124,426	5.324
9	Charleston - Jacksonville	62,731,185	184.469	107,322	6.097
10	Charleston - Norfolk	63,184,050	186.153	560,187	7.781
11	Charlotte - Columbus	63,148,713	192.806	524,851	14.434
12	Charlotte - Norfolk	63,113,170	184.121	489,307	5.749
13	Chicago - Cleveland	62,791,334	184.749	167,472	6.377
14	Chicago - Detroit	63,181,462	183.607	557,599	5.235
15	Chicago - Indianapolis	63,366,856	184.898	742,994	6.526
16	Chicago - Pittsburgh	63,568,431	185.842	944,569	7.470
17	Cleveland - Columbus	63,151,184	185.864	527,322	7.492
18	Cleveland - New York	62,902,990	187.062	279,127	8.690
19	Cleveland - Pittsburgh	63,355,890	183.269	732,027	4.897
20	Columbus - Detroit	63,181,501	187.682	557,639	9.309
21	Columbus - Indianapolis	62,907,744	189.678	283,881	11.306
22	Columbus - Norfolk	62,703,766	184.149	79,903	5.777
23	Detroit - Nashville	62,836,195	183.546	212,332	5.174
24	Indianapolis - Nashville	63,301,108	184.366	677,245	5.994
25	Indianapolis - Norfolk	62,730,086	184.251	106,223	5.879
26	Indianapolis - St. Louis	62,742,049	183.490	118,187	5.117
27	New York - Philadelphia	62,763,407	183.698	139,544	5.326

Table 6: Post-disruption objective function values (terminals)

No.	Terminal	Total Cost	Total Risk	Cost Increase	Risk Increase
1	Atlanta	63,581,241	177.132	957,378	-1.239
2	Baltimore	65,223,236	179.268	2,599,373	0.896
3	Charleston	62,893,928	180.165	270,065	1.793
4	Charlotte	62,912,715	183.904	288,852	5.532
5	Chicago	64,693,587	176.831	2,069,724	-1.540
6	Cleveland	64,620,267	183.766	1,996,405	5.394
7	Columbus	63,006,900	184.269	383,038	5.897
8	Detroit	64,180,308	181.642	1,556,445	3.270
9	Indianapolis	63,106,983	183.716	483,121	5.344
10	Jacksonville	62,697,925	179.334	74,063	0.962
11	Nashville	63,372,036	178.662	748,173	0.290
12	New York	62,593,026	181.293	-30,836	2.921
13	Norfolk	62,540,241	183.181	-83,620	4.808
14	Philadelphia	63,075,336	184.730	451,474	6.358
15	Pittsburgh	62,821,773	182.364	197,910	3.992
16	St. Louis	62,742,049	183.490	118,187	5.117

As is evident from Table 5, the disruption of the Baltimore-Pittsburgh service leg has the highest impact in terms of cost. This can be attributed to the high utilization rate of this service leg in the base-case solution as evidenced by Figure 3. Since a large number of containers need to be rerouted to costlier paths, the overall cost of operations increases significantly. Similarly, a disruption in the Baltimore terminal leads to a substantial surge in total

cost. The highest increase in risk occurs after a disruption in the Charlotte-Columbus service leg, and the Philadelphia terminal which are both used in a large number of least risk paths.

As we mentioned in Section 3.1, the purpose of obtaining these numerical values representing the increase or decrease in post-disruption objective function values is to use them as input for the subsequent machine learning models. Each row in Tables 5 and 6, which represents the post-disruption impact of a service leg or a terminal respectively, will be regarded as an input data point. This provides us with 27 data points in the service leg data set and 16 data points in the terminal data set which are clearly not enough to train a generalizable classification model.

Therefore, we assume the demand data for 10 additional planning periods are available and we go through the process outlined in the beginning of this section to obtain the results in Tables 5 and 6 for each subsequent planning period. It is worthy to note that the total number of containers to be transported in each subsequent period varies between 19,000 and 21,000 containers and customer demand will be randomly assigned to each traffic-class. In addition to providing us with 297 data points in the service legs data set and 176 data points in the terminals data set, this provision ensures that variability in real life transportation demand is also incorporated in our analysis.

Chapter 6

Predictive analytics

The transportation company decision-makers can identify the infrastructure with the highest negative impact on total cost and/or risk by looking at the results of the post-disruption model summarized in Tables 5 and 6. For instance, it is clear from column five of Table 5 that a disruption in the Atlanta-Nashville service leg causes a massive increase in cost of more than two million dollars while a disruption in Charlotte-Columbus does not increase the cost as much but increases the population at risk by more than 14 people. The Baltimore-Pittsburgh service leg increases network-wide costs by more than two million and also increases total risk to the population by more than 11 individuals.

With regards to terminals, a disruption in the Baltimore intermodal terminal results in an increase of more than 2.5 million dollars, while a disruption in the Philadelphia intermodal terminal increases the network-wide risk

by more than 6 individuals. Cleveland terminal's disruption is impactful in terms of both objectives with close to 2 million dollars in cost increase, and exposing an additional 5 people to the risk of death or serious injury.

Although comparing the actual post-disruption total cost and risk impact values can be useful in accurately identifying the critical infrastructure, obtaining these values is computationally expensive and time-consuming, since the routing optimization model needs to be solved for as many times as the number of service legs and terminals in the network. Consequently, the bigger the network is, the less efficient this method of obtaining actual post-disruption values and then manually categorizing the infrastructure becomes.

Our proposed methodology's advantage lies within its promise to help the decision-makers circumvent the process of obtaining actual post-disruption total cost and risk impact values for every single transportation planning period, once a reliable classification model has been trained. The goal of categorizing the company's infrastructure into different classes based on their post-disruption impact on network performance is realized through harnessing the power of a category of unsupervised learning techniques known as clustering which will aid us in categorizing network elements, as well as supervised learning techniques known as classification which will assign the infrastructure to the pertinent criticality class based on a predefined set of their features.

6.1 Clustering

In order to plan for disruption mitigation strategies, the transportation company's decision-makers need to have a clear idea of which subset of their network infrastructure can be considered high impact and which ones can be considered low impact, since applying the same mitigation strategies to all the service legs and terminals will be very costly and not economically viable. This is an area in which clustering techniques can be very helpful.

Clustering refers to a host of techniques for discovering subsets or groups of similar observations in a data set. The aim of this process is to divide the data points into groups in which members are as similar to each other as possible, while data points belonging to different groups should be quite dissimilar to each other. The measure of similarity in our case is the amount of increase in the post-disruption total cost and/or total risk compared to the pre-disruption total cost and total risk. In other words, we want the network infrastructure pieces which lead to significant increases in post-disruption cost and/or risk when disrupted to be grouped together, and the ones which lead to smaller negative impacts to be placed into other groups.

One of the most commonly used and convenient clustering techniques is the K-means clustering algorithm. James et al. (2013) state that K-means

clustering minimizes within-cluster variances or the sum of squared Euclidean distance from every data point to the centroid in a cluster, and define it as the following optimization problem (equation from James et al. (2013)):

$$\underset{C_1,\ldots,C_K}{minimize} \left\{ \sum_{k=1}^{K} \frac{1}{|C_k|} \sum_{i,i' \in C_k} \sum_{j=1}^{p} (x_{ij} - x_{i'j})^2 \right\} \tag{5}$$

in which K is the number of clusters, $|C_k|$ signifies how many data points are in the kth cluster and x_{ij} are the data points in the kth cluster.

In K-means clustering, the data points are partitioned into a predefined number of clusters; therefore, we need a method to determine the number of clusters that works best for our data set. The Silhouette Coefficient method and the Elbow Criterion method are two commonly used methods that aid us in selecting the optimal number of clusters.

In the elbow criterion method, the underlying idea is to run the K-means algorithm on the data set for a specified range of k values and plot the resulting within-cluster sum of squares (WCSS) against the number of clusters. The elbow of the resulting curve in the graph will be chosen as the optimal number of clusters since the diminishing returns after this point makes picking a higher number of clusters not worth the additional cost. The goal in the elbow criterion method is to adopt a small number of clusters that entails a reasonably small sum of squared distances between different data points in a cluster.

In the silhouette coefficient method, the silhouette coefficient/score is a measure of how similar a data point is to other points in the same cluster and how dissimilar it is to data points in the neighboring cluster. Silhouette score can take values between -1 and +1, with the former representing wrong clustering for a data point and the latter representing accurate clustering. Therefore, the average silhouette score, which is the mean of the silhouette scores of individual data points in the data set, can signify how good the clustering performance for a specific number of clusters has been.

Having obtained the optimal number of clusters by utilizing these techniques, we run the K-means clustering algorithm on our data set to assign every service leg and terminal to a cluster. This categorization will be regarded as the correct class of post-disruption objective function impact (criticality class) of a network element and will be used as the response variable for the training of our subsequent classification model. The results of our clustering analysis will be presented in the following sections.

It should be noted that the K-means clustering algorithm and the pertinent analysis done in this study were implemented using the functions available in Python's Scikit-learn library version 0.22.1 (Pedregosa et al., 2011).

6.1.1 Clustering of service legs

In order to implement the K-means clustering algorithm for the service legs, we pool all the 297 data points that we obtained by calculating the increase in total cost and total risk due to disruption on a service leg for all the 11 transportation planning periods considered in our study. This data aggregation provides more input data points for the clustering algorithm which in turn improves its performance.

The resulting data set is two-dimensional meaning that each data point has two attribute values. The first dimension signifies the increase in post-disruption cost for a particular service leg (see column five of Table 5), and the second dimension signifies the increase in post-disruption risk for the same service leg (see column six of Table 5).

Figure 6 depicts a scatter plot of the 297 data points with the increase in cost represented on the x-axis and the increase in risk represented on the y-axis and each point representing a service leg in one of the 11 transportation planning periods. We can already see that some data points are closer to each other and can potentially be clustered into the same group. Therefore, Figure 6 can be utilized to validate the results of the K-means clustering algorithm as well as gaining more insight about the resulting clusters.

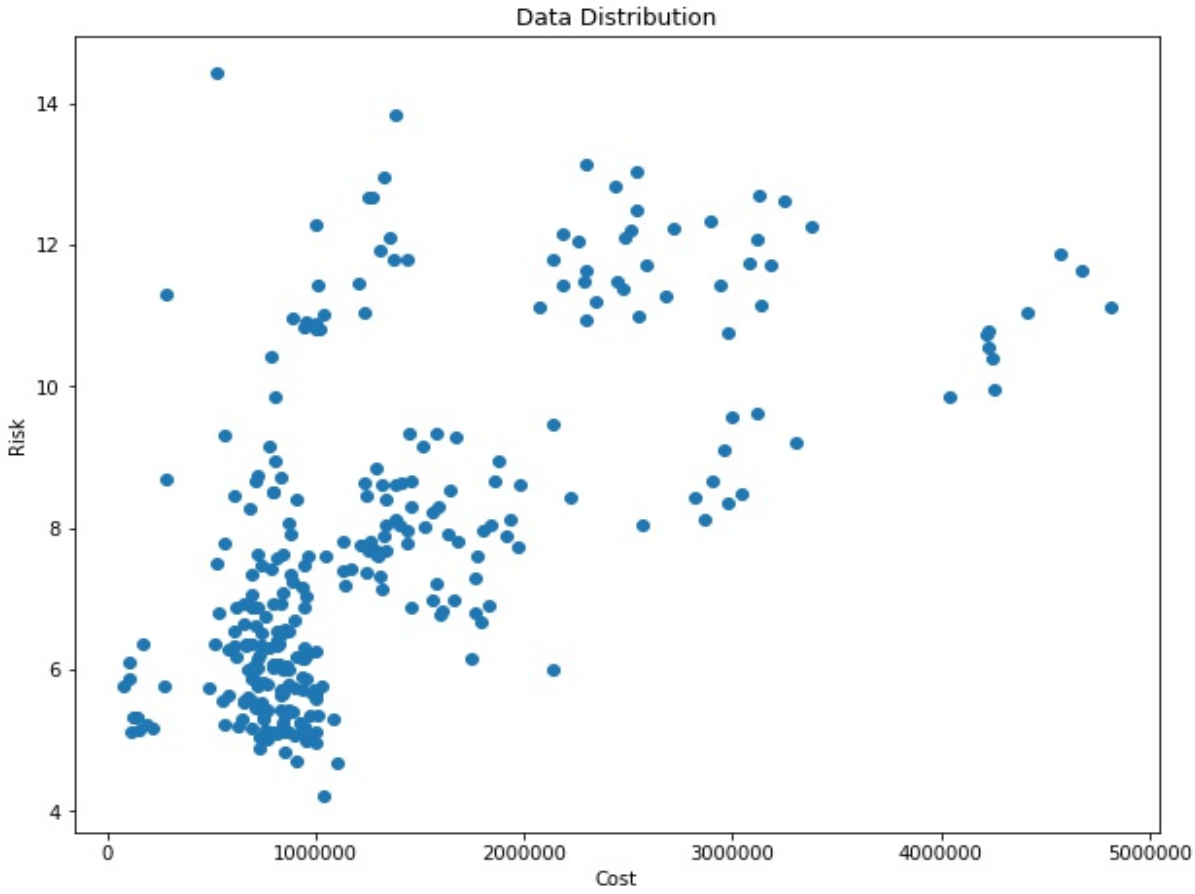

Figure 6: Distribution of disruption impact data (service legs)

The next step is to find the optimal number of clusters for this data set. As mentioned in the beginning of this chapter, we will use the average silhouette score and the elbow criterion method to achieve this goal. We enlist the aid of Figure 7, which is a visual representation of the results of these two methods, and Table 7 to explain how we obtain the optimal number of clusters via these methods.

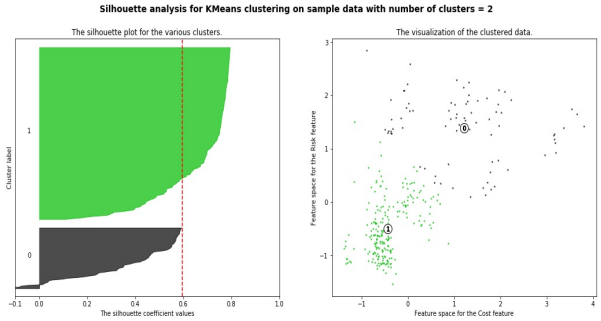

(a) No. of Clusters = 2

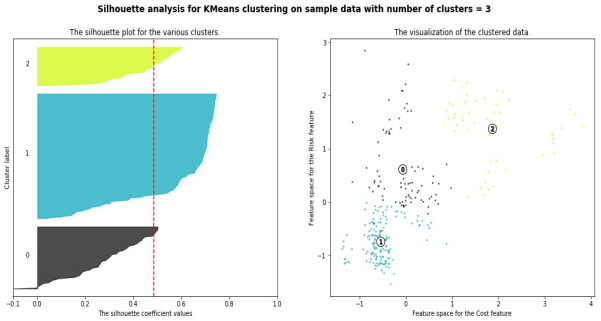

(b) No. of Clusters = 3

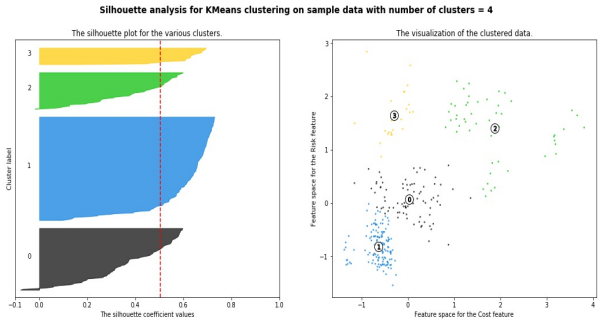

(c) No. of Clusters = 4

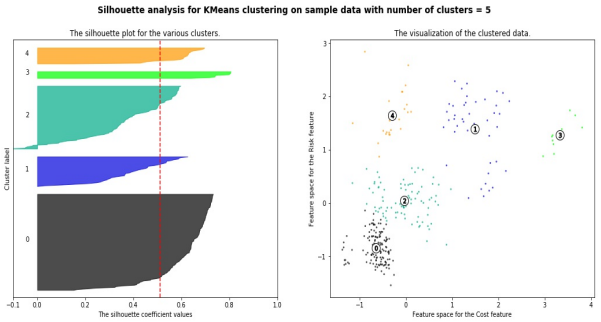

(d) No. of Clusters = 5

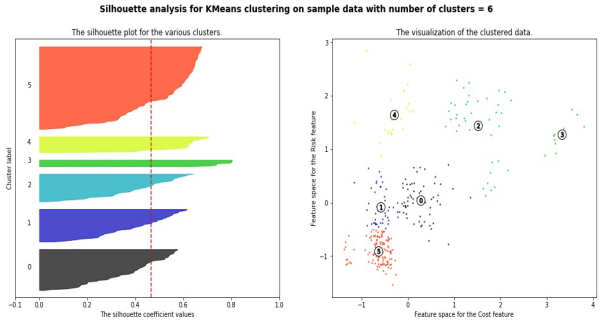

(e) No. of Clusters = 6

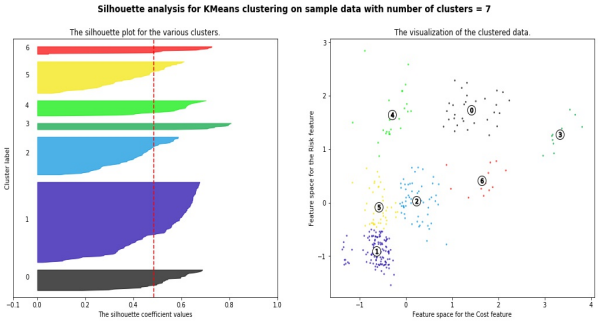

(f) No. of Clusters = 7

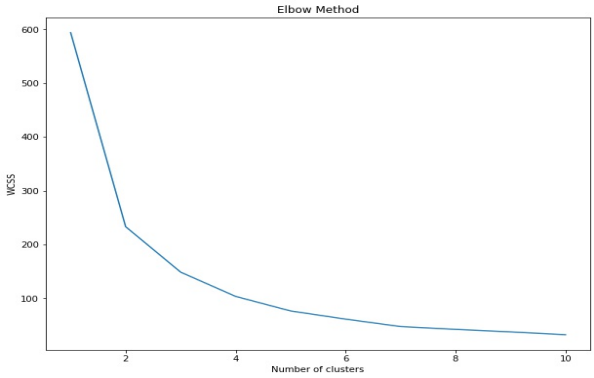

(g) The elbow plot

Figure 7: Silhouette plots and the elbow plot (service legs)

In parts (a) to (f) of Figure 7, the silhouette score for every data point is represented on the x-axis of the left-hand side figure, while the different clusters are represented on the y-axis and highlighted with a distinct color. The vertical red lines in the same figures represent the average value of all the data points' silhouette scores obtained after running the K-means algorithm with the corresponding number of clusters. The right-hand side figures in parts (a) to (f) are scatter plots of the data points that highlight the results of running the clustering algorithm with the corresponding number of clusters as well as the ensuing cluster centers. Each cluster's members are highlighted in the same color used in the left-hand side figure to illustrate the silhouette scores.

To further clarify the intricacies of these figures, we turn our attention to part (c) of Figure 7. It depicts the silhouette scores obtained after running the clustering algorithm with 4 clusters. We can observe that most of the data points in the blue cluster have high silhouette scores which signifies a good clustering performance, while the green cluster's data points mostly have low silhouette scores which is a sign of poor clustering results. We can observe this more intuitively in the right-hand side figure. The data points in the blue cluster are substantially closer to each other than the data points in the green cluster. Hence, the optimal number of clusters will most probably not be equal to four for this data set.

In part (g), we have the elbow plot with the within-cluster sum of squares (WCSS) on the vertical axis and the number of clusters on the horizontal axis. As the number of clusters increases, the within-cluster sum of squares decreases until it reaches a value of zero when the number of clusters equals the number of observations in the data set.

By looking at Table 7, we can see that the best average silhouette score belongs to $k = 2$; however, since the within-cluster sum of squares is a rather large value, running the algorithm with just two clusters will not yield an ideal result. As mentioned before, the goal is to choose a small k as long as it produces a reasonably small within cluster sum of squares. The next best average silhouette score belongs to k = 5 and we can see that the corresponding within-cluster sum of squares is adequately small as well. Therefore, we pick $k = 5$ as the optimal number of clusters.

Table 7: Performance of different cluster numbers (service legs)

Number of Clusters	Average Silhouette Score	Within Cluster Sum of Squares
k = 2	0.594	233.090
k = 3	0.485	148.562
k = 4	0.505	103.338
k = 5	0.512	76.303
k = 6	0.465	61.118
k = 7	0.484	47.277

Ultimately, we run the K-means clustering algorithm with number of clusters set to be five. Figure 8 illustrates the results of our clustering model, with data points in the same cluster represented with a unique color and cluster centers represented with a red circle. It should also be noted that since the K-means algorithm is sensitive to the scale of Euclidean distances between data points, we need to scale the data set along its two dimensions before running the model, considering the fact that the values associated with increase in post-disruption total cost are several orders of magnitude higher than the values associated with increase in post-disruption total risk.

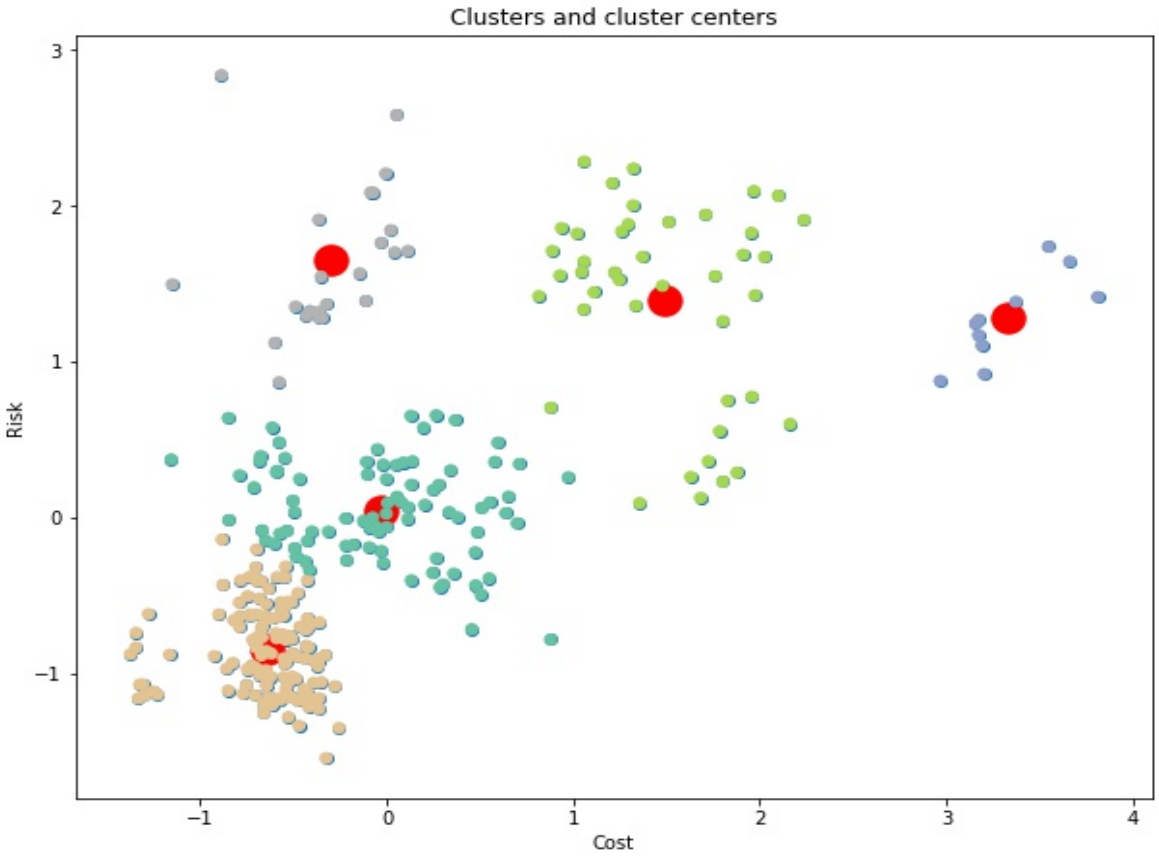

Figure 8: Service legs clustering results

As is evident from Figure 8, majority of service legs in a cluster increase total cost and risk more or less than a specific amount which is the basis of grouping data points in the clustering algorithm. The attributes of these clusters have been further elaborated in Table 8. We have also assigned each of these clusters a name that underlines their respective attributes. These cluster names will be used as the true label of each service leg in the subsequent classification models.

Table 8: Service legs cluster attributes

Cluster Color	Cluster Name	Attributes
Purple	Steep Cost & Risk Impact	Majority of service legs in this cluster increase the total cost by more than 4 million dollars and total risk by more than 10 persons
Green	High Cost & Risk Impact	Majority of service legs in this cluster increase total cost by more than 2.2 million dollars and total risk by more than 8 individuals
Gray	Steep Risk Impact	Majority of service legs in this cluster increase total risk by more than 11 individuals, while total cost increase is less than 1.5 million dollars
Teal	Moderate Cost & Risk Impact	Majority of service legs in this cluster increase the total cost by less than 2 million dollars and total risk by more than 9 persons
Hazel	Low Cost & Risk Impact	Majority of service legs in this cluster increase the total cost by less than 1 million dollars and total risk by more than 7 persons

6.1.2 Clustering of terminals

Due to the fact that the process of implementing the K-means clustering algorithm on the terminals data set is the same as the process implemented for the service legs data set and in the interest of brevity, we will refrain from going into too much detail in this section and instead, only a brief description of each step and the obtained results will be presented.

The first step involves pooling all the 176 data points that we have procured by calculating the increase in total cost and total risk due to disruption on a service leg for all the 11 transportation planning periods considered in our study. Combining the data from several transportation periods provides more input data points for the clustering algorithm which subsequently leads to a clustering performance improvement.

The 176 data points are drawn in the scatter plot illustrated in Figure 9, with increase in post-disruption total risk on the vertical axis and increase in post-disruption total cost on the horizontal axis, while each point represents a terminal in one of the 11 transportation planning periods. The result is a visual representation of this two-dimensional data set that will aid us in validating the performance of the K-means clustering algorithm, as well as gaining some insight into the characteristics of the possible clusters.

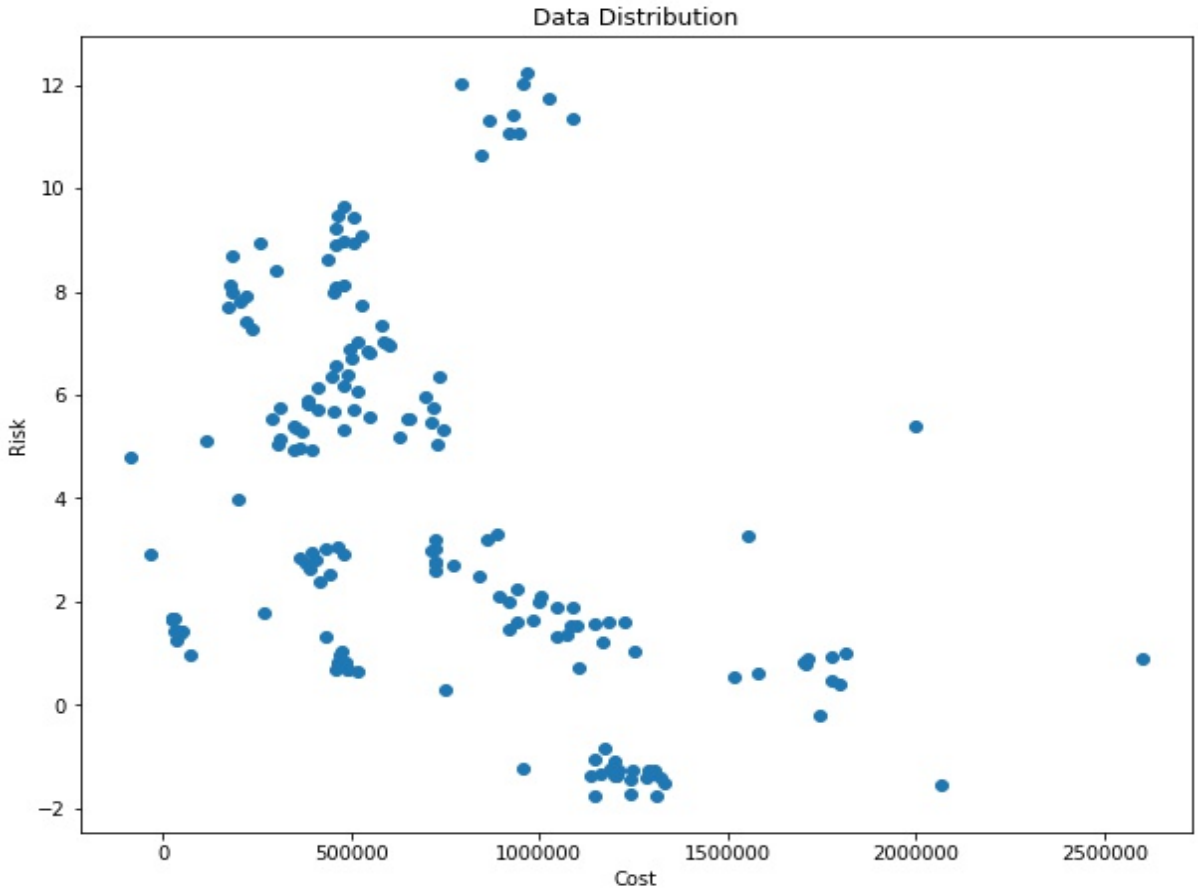

Figure 9: Distribution of disruption impact data (terminals)

The next task is to find the optimal number of clusters for the K-means algorithm. Once again, we utilize the silhouette coefficient and the elbow criterion methods to obtain the optimal number of clusters. We plotted and analyzed the silhouette scores and the associated clustering results for k ranging from 2 to 7 in parts (a) to (f) of Figure 10. Moreover, we plotted the within-cluster sum of squares against number of clusters ranging from 1 to 10 and produced the graph known as the elbow plot in part (g) of Figure 10.

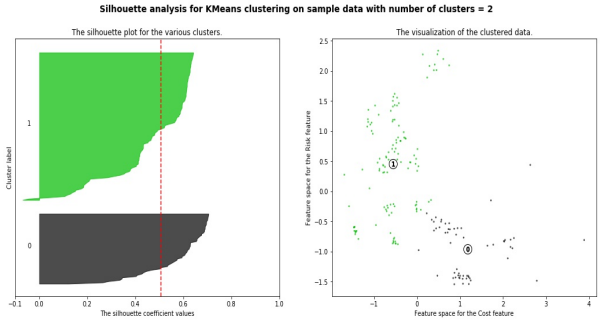

(a) No. of Clusters = 2

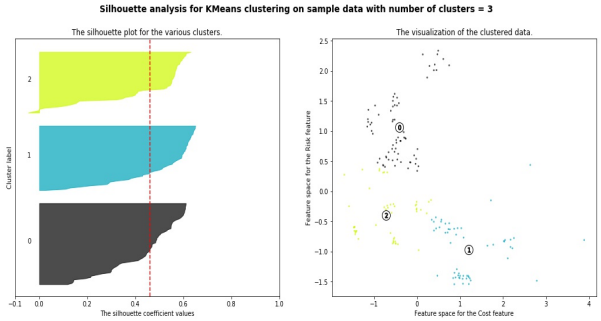

(b) No. of Clusters = 3

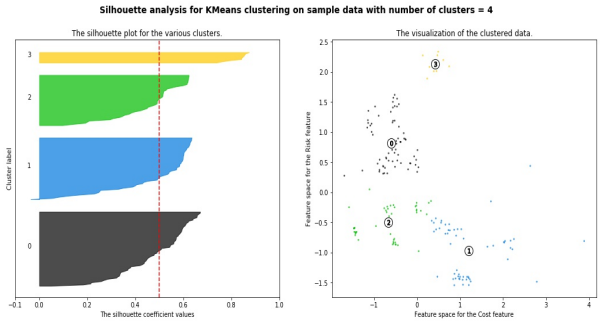

(c) No. of Clusters = 4

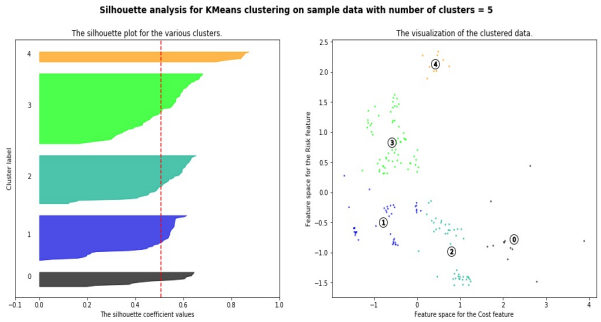

(d) No. of Clusters = 5

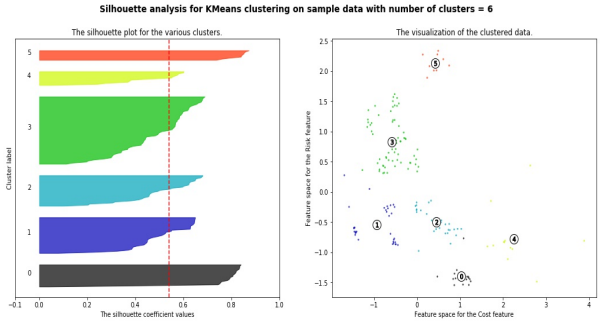

(e) No. of Clusters = 6

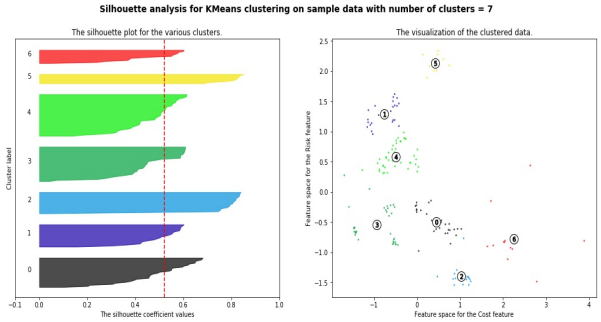

(f) No. of Clusters = 7

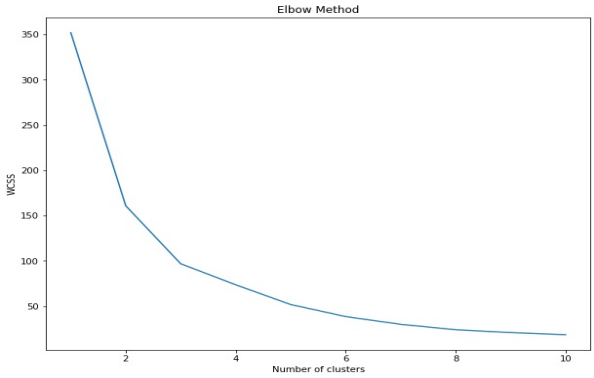

(g) Elbow plot

Figure 10: Silhouette plots and the elbow plot (terminals)

The plots in Figure 10 and their significance have been explained in more detail in the service legs clustering section.

Table 9 contains average silhouette scores and within cluster sum of squares (WCSS) for number of clusters (k) ranging from 2 to 7. The highest average silhouette score recorded in the table belongs to k = 6 and the corresponding within-cluster sum of squares is also reasonably small; therefore, the conditions for choosing 6 as the ideal number of clusters are met. It is also worthy to note that the within cluster sum of squares will eventually be zero when the number of clusters is equal to the number of observations in the data set. However, by looking at the elbow plot we can see that the WCSS doesn't decrease significantly after k = 6 and thus, it is not worth the extra cost to reduce the WCSS further. Moreover, increasing k beyond a certain value may lead to potential difficulty in analyzing and justifying the clustering results.

Table 9: Performance of different cluster numbers (terminals)

Number of Clusters	Average Silhouette Score	Within Cluster Sum of Squares
k = 2	0.506	160.785
k = 3	0.461	96.701
k = 4	0.498	73.532
k = 5	0.507	51.745
k = 6	0.539	38.436
k = 7	0.522	29.887

Running the K-means clustering algorithm with six as the optimal number of clusters for the terminal data set produces the clusters illustrated in Figure 11. Each of these clusters has been drawn with a different color and the cluster centers are represented by relatively bigger red points in the aforementioned figure. It is worthy to note that due to the sensitivity of the K-means clustering algorithms to the Euclidean distances between data points, the data set has been scaled and the values on the x-axis and the y-axis are the scaled versions of original values.

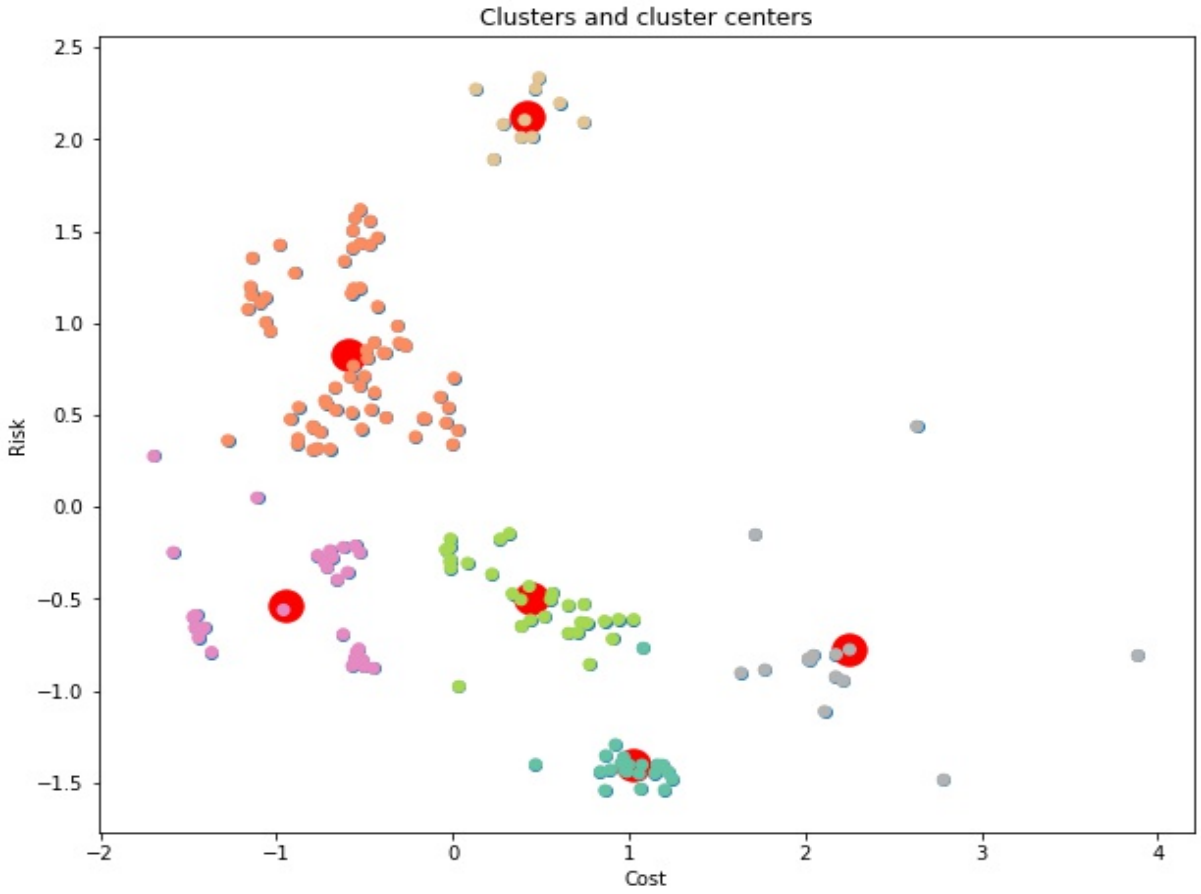

Figure 11: Terminals clustering results

The attributes of clusters obtained using the K-means algorithm have been summarized in Table 10. Moreover, each cluster has been assigned a name that will be used as the true label for each of its member data points in the training and testing of subsequent classification models.

Table 10: Terminals cluster attributes

Cluster Color	Cluster Name	Attributes
Gray	Steep Cost Impact	Majority of service legs in this cluster increase the total cost by more than 1.5 million dollars but total risk does not increase significantly
Teal	High Cost Impact	Terminals in this cluster increase total cost on average by approximately 1.25 million dollars but they decrease total risk by a small margin
Green	Moderate Cost & Risk Impact	Terminals in this cluster increase total cost on average by roughly 1.5 million dollars, while total risk increase is on average approximately 2 individuals
Purple	Low Cost & Risk Impact	Majority of terminals in this cluster increase the total cost by less than half a million dollars and total risk by less than 3 persons
Orange	High Risk Impact	Terminals in this cluster increase total risk by around 7 persons and total cost by around half a million on average
Hazel	Steep Risk Impact	Terminals in this cluster increase total risk by more than 11 persons and total cost by around 1 million dollars on average

6.2 Classification

Classification, an instance of supervised learning, is the process of determining to which class or category an unknown observation belongs by utilizing a classification model trained on a set of data with known classes. In the context of our study, we are interested in knowing to which class of post-disruption cost and/or risk impact, an unknown service leg or terminal belongs and we hope to perform this task by developing and using a classification model that boasts high accuracy.

Developing a classification model requires a training set with known labels as well as a set of input features that facilitate the creation of a model for the relationship between predictors commonly denoted by X and the response variable commonly denoted by Y. We have already created a data set with labeled observations in the previous section. Consequently, we need to identify a set of features that will have a significant relationship with the label variable.

The features that we use in the following classification models are a mixture of features extracted from the results of the mathematical optimization model and features that are based on the transportation network's topology. We will explain the selected features for service legs and terminals separately in the following subsections. The next logical step would be to assess whether

the features improve the fit of the model. The features that contribute to improving the fit of the model will be kept in the model while the rest will be discarded. To be able to evaluate the model, we will set aside 10 percent of the observations in the data set and call it the test set, and the remaining 90 percent of data points will act as the classification model's training set. Ultimately, several different classification algorithms as outlined below will be implemented on this study's data sets.

Now we will turn our attention to providing a brief and intuitive explanation of each classification technique based on the definition presented in James et al. (2013) and the relevant literature. We also invite the reader to refer to James et al. (2013) for a more in depth review of the supervised learning techniques used in this study.

The bagging, boosting and random forests algorithms use decision trees as a stepping stone toward building better predictive models. In the decision tree classifier, the algorithm starts at the root and repeatedly partitions the data points based on the feature that may best divide the data. Gradient boosting uses a weak learner like decision trees to fit an initial model to the data set. Each successive model that is added tries to improve on the shortcomings of the previous model and thus an ensemble of predictive models is created. Bagging classifier uses the concept of bootstrap to extract multiple samples from the

training data set and by taking the average of the predictions, decreases the variance of decision tree models. To improve classification performance, the random forests classifier decreases correlation in the trees by only allowing a random subset of features to be considered at each tree partition.

The goal of the support vector classifier is to create hyperplanes or boundaries based on which the data points will be classified. Neural networks, which are a set of neurons arranged in layers, learn by creating weighted associations between an example input and output and recursively adjusting the weightings such that the result of their layered processing becomes more like the ideal output. Independence between the features and Gaussian distribution in the training data set is assumed in the Gaussian naive Bayes classifier, and the Bayes theorem is used to classify the data points. Linear discriminant analysis makes predictions based on estimating the probability of a data point belonging to each of the existing classes in the data set. In the k-nearest neighbor algorithm, an unknown observation will be assigned to the class which has the most representatives in the neighborhood of size k around the data point.

It should be noted that all classification algorithms and the pertinent analysis in this study were implemented using the functions available in Python's Scikit-learn library version 0.22.1 (Pedregosa et al., 2011).

6.2.1 Service legs classification models

The first task in the implementation of classification models on the service legs is to identify a set of service leg features with potential relationship with the label variable. The routing optimization model introduced in Section 4.1, provides us with five service leg features that have the potential to be used as input for the classification models. For instance, we will extract the optimal number of regular containers on each service leg from the results of the optimization model to be used as a feature in the training and testing of classification models. Another service leg feature obtained from the results of the optimization model is the optimal number of trains that traverse that specific service leg. The first five features explained in Table 11 refer to these input features.

The next six features are based on the topological properties of the company's transportation network as opposed to its supply and demand aspects. Some of these features have been adopted from relevant literature and others have been inspired by concepts in graph theory. For instance, the number of times a service legs is used in the least cost paths for all the traffic-classes can be considered a service leg feature. Another possible feature is the number of adjacent service legs. The last six features explained in Table 11 refer to these input features.

This will provide the classification model with eleven input features in total, an overview of which is presented in Table 11. It is worthy to mention that a direction for feature research can be trying to identify other service leg features and incorporating them in the analysis .

Table 11: Input features for the classification model (service legs)

Feature No.	Feature Name	Explanation
1	Regular Opt Vol	Optimal volume of regular containers
2	Class 2 Opt Vol	Optimal volume of class 2 hazmat containers
3	Class 3 Opt Vol	Optimal volume of class 3 hazmat containers
4	Class 8 Opt Vol	Optimal volume of class 8 hazmat containers
5	Number of Trains	Optimal number of trains traversing a service leg
6	Path Contribution	The number of times a service leg is used in the feasible paths of the network
7	Cost Profile	The number of times a service leg is used in the network's least cost paths
8	Class 2 Risk Profile	The number of times a service leg is used in the network's Class 2 least risk paths
9	Class 3 Risk Profile	The number of times a service leg is used in the network's Class 3 least risk paths
10	Class 8 Risk Profile	The number of times a service leg is used in the network's Class 8 least risk paths
11	Adjacent Service Legs	Number of direct connections to other service legs

Table 12 contains common descriptive statistics such as minimum, maximum, mean and standard deviation for each of the features discussed.

Table 12: Descriptive statistics for input features (service legs)

No.	Name	Format	Min	Max	Mean	Std Dev
1	Regular Opt Vol	Numeric	2	2960	822.29	568.89
2	Class 2 Opt Vol	Numeric	0	721	229.97	178.86
3	Class 3 Opt Vol	Numeric	0	1131	382.21	298.17
4	Class 8 Opt Vol	Numeric	0	452	149.82	114.73
5	Number of Trains	Numeric	2	42	19.09	11.38
6	Path Contribution	Numeric	1728	7326	4020	1309.14
7	Cost Profile	Numeric	0	108	36.7	27.6
8	Class 2 Risk Profile	Numeric	0	116	36.29	29.89
9	Class 3 Risk Profile	Numeric	0	118	36.37	30.22
10	Class 8 Risk Profile	Numeric	0	119	33.77	31.35
11	Adjacent Serv Legs	Numeric	2	9	5.7	1.86

The next step is to evaluate each feature's potential contribution or lack thereof to improving the fit of the model. Using Scikit-learn's ANOVA F-test, which is commonly used for identifying the best input features of a classification model, we obtain the pertinent p-values for each feature. In case the obtained p-value is less than the predefined significance level, we will be able to reject the relevant null hypothesis and keep the aforementioned feature as an input for the model.

In order to better understand the significance of each feature to the fit of the model, we have plotted $-Log(p-value)$ of each feature in a bar chart illustrated in Figure 12. The red line represents our chosen significance level.

As is evident from the figure, all of the selected features have p-values that are substantially less than the our adopted significance level of $\alpha = 0.05$ and therefore, we can keep and utilize all of them in the model.

However, in case the performance of classification models are not satisfactory, we can remove the features that do not contribute as much to the fit of the model by only including the ones with the best performance in the F-test in the model. Another popular technique that can be used in such circumstances is the Principal Component Analysis which can significantly increase the accuracy of classification models on some data sets (James et al., 2013).

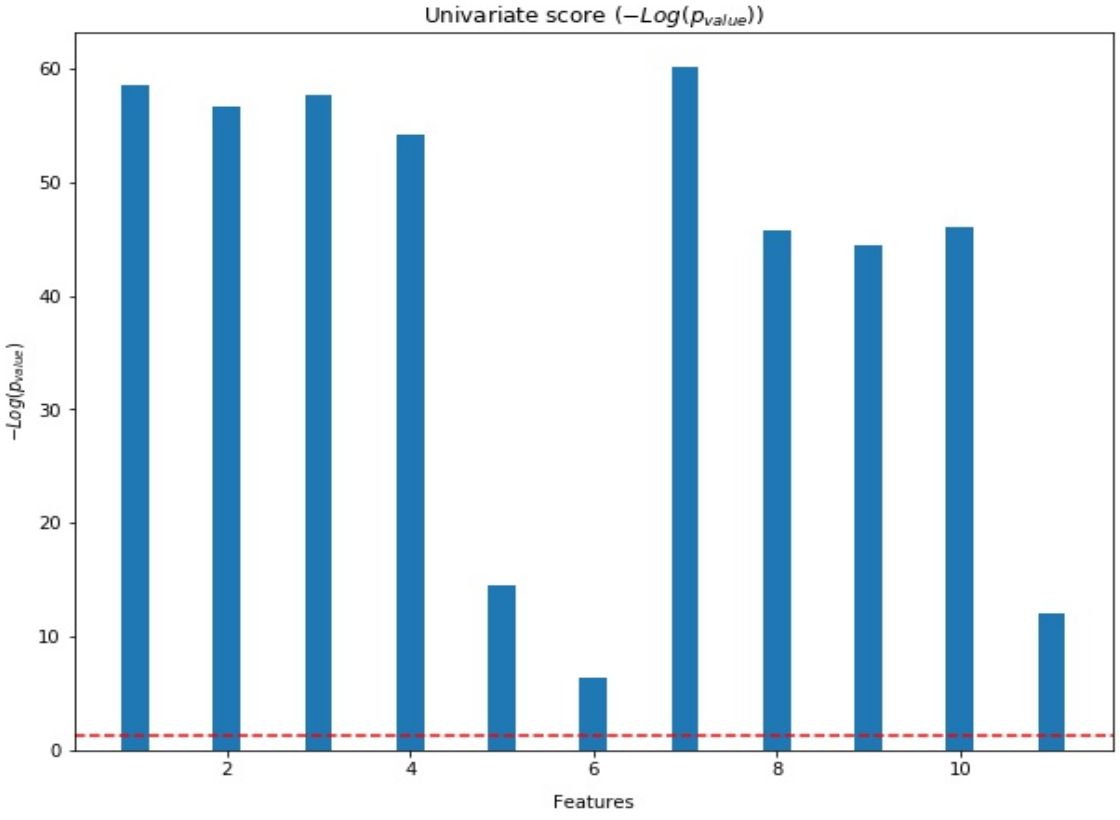

Figure 12: Significance of service leg input features

The final task is to train the classification model using the the chosen algorithms i.e. support vector classifier, k-nearest neighbors, etc. and evaluate their accuracy. Accuracy of a classification model refers to how often it correctly classifies the data points or in this case, the percentage of service legs that are assigned to the correct class. The highest accuracy reached is 93% which is a relatively excellent performance for a classification task. Table 13 summarizes the accuracy of the nine classification algorithms implemented along with a visual representation of each model's confusion matrix.

The confusion matrix is a special table that facilitates the visualization of a classification algorithm's performance. The name originates from the fact that this visual matrix enables us to see if the model is confusing two or more classes. Each row in the confusion matrix signifies data points in one of the true classes and each column signifies data points in one of the predicted classes. Therefore, if a data point in the test set is classified correctly, it will be located on the diagonal of the confusion matrix. For instance, the yellow box in the support vector machine's confusion matrix represents around 12 service legs belonging to the class denoted by zero that have been classified correctly. However, there are two off-diagonal boxes as well that represent service legs belonging to the class denoted by two that have been incorrectly classified into classes denoted by zero and one.

Table 13: Performance of classification models (service legs)

Support Vector Classifier	Neural Network	K-Nearest Neighbors
Accuracy: 93.3%	Accuracy: 93.3%	Accuracy: 93.3%
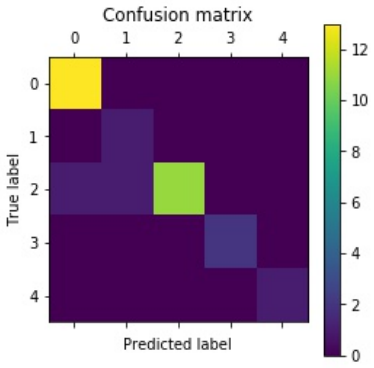	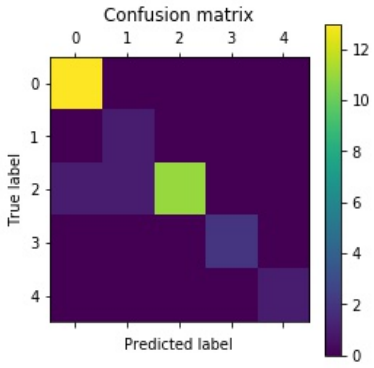	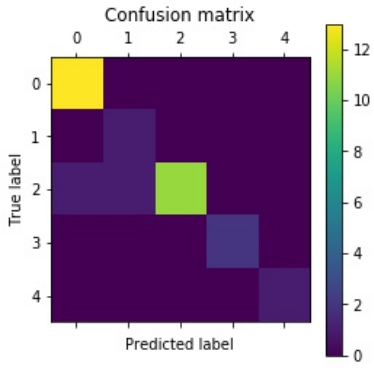
Decision Tree Classifier	**Random Forests**	**Bagging**
Accuracy: 90%	Accuracy: 93.3%	Accuracy: 90%
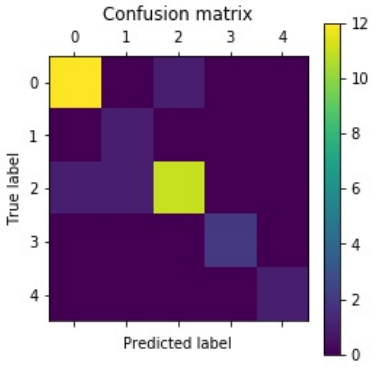	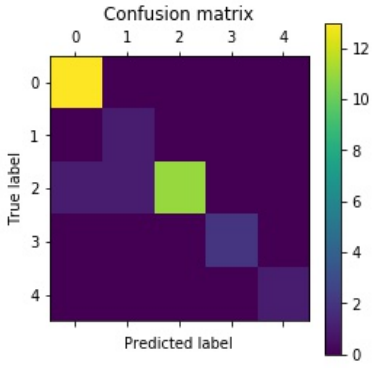	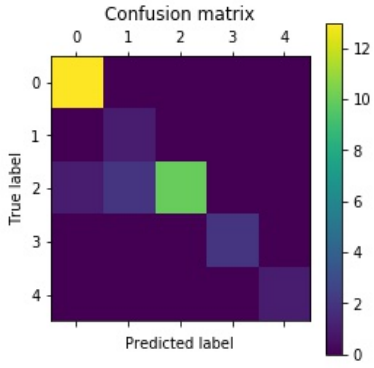
Gradient Boosting	**Linear Discriminant Analysis**	**Gaussian Naive Bayes**
Accuracy: 93.3%	Accuracy: 80%	Accuracy: 66.6%
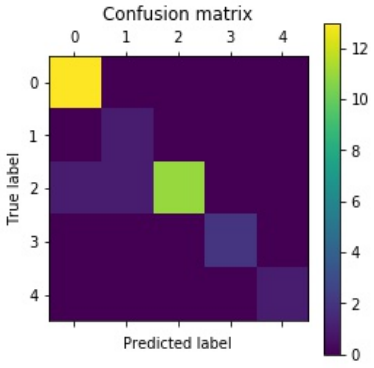	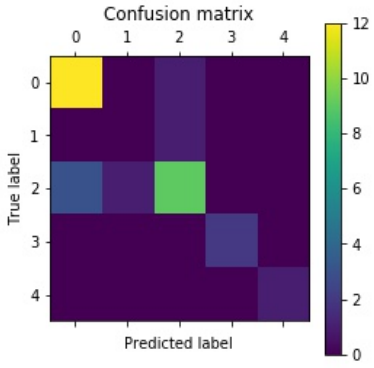	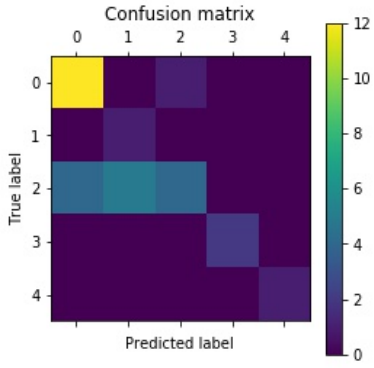

6.2.2 Terminals classification models

Similar to the process we followed through for the service legs, the first task in the process of building a classification model for terminals is identifying a set of features (predictors) with potential relationship with the response variable. We identified 10 features in total for each intermodal terminal and these features have been further explained in Table 14.

Table 14: Input features for the classification model (terminals)

Feature No.	Feature Name	Explanation
1	Regular Opt Vol	Optimal volume of regular containers
2	Class 2 Opt Vol	Optimal volume of class 2 hazmat containers
3	Class 3 Opt Vol	Optimal volume of class 3 hazmat containers
4	Class 8 Opt Vol	Optimal volume of class 8 hazmat containers
5	Path Contribution	The number of times an intermodal terminal is used in the feasible paths of the network
6	Cost Profile	The number of times an intermodal terminal is used in the network's least cost paths
7	Class 2 Risk Profile	The number of times an intermodal terminal is used in the network's Class 2 least risk paths
8	Class 3 Risk Profile	The number of times an intermodal terminal is used in the network's Class 3 least risk paths
9	Class 8 Risk Profile	The number of times an intermodal terminal is used in the network's Class 8 least risk paths
10	Degree Centrality	Number of links (service legs) in the network connected to this intermodal terminal

The first four variables are based on the routing optimization model introduced in Section 4.1. These four features are identical to the ones used for service legs except for the fact that we calculate the number of containers that are transferred from truck to train or vice versa in this terminal, instead of the ones traversing service legs. The other six features are based on the topological properties of the company's transportation network. These features have been inspired either by ideas from graph theory or by features used in relevant literature. For instance, the concept of degree centrality for a node which in this context means the number of service legs that are directly connected to a terminal has been adopted from graph theory.

Table 15 contains common descriptive statistics such as minimum, maximum, mean and standard deviation for each of the features discussed.

Table 15: Descriptive statistics for input features (terminals)

No.	Name	Format	Min	Max	Mean	Std Dev
1	Regular Opt Vol	Numeric	111	2889	1250	566.93
2	Class 2 Opt Vol	Numeric	85	676	375.38	122.55
3	Class 3 Opt Vol	Numeric	103	1081	622.82	204.67
4	Class 8 Opt Vol	Numeric	68	419	251.78	69.72
5	Path Contribution	Numeric	4104	5472	4387.5	522.91
6	Cost Profile	Numeric	12	96	54	23.55
7	Class 2 Risk Profile	Numeric	2	90	54	28.14
8	Class 3 Risk Profile	Numeric	2	90	54	28.25
9	Class 8 Risk Profile	Numeric	18	90	54	25
10	Degree Centrality	Numeric	1	6	3.37	1.26

The next step is to evaluate each feature's contribution or lack thereof to improving the fit of the model. Implementing the ANOVA F-test, which is commonly used for identifying the best input features of a classification model, we extract the pertinent p-values for each feature. As was mentioned before, if the p-value for a feature is less than the predefined significance level, we will be able to reject the relevant null hypothesis and keep that feature in the model.

In order to better understand the significance of each feature for improving the fit of the model, we have plotted $-Log(p-value)$ of each feature in a bar chart illustrated in Figure 12. The red line represents the chosen significance level. As is evident from the figure, all of the selected features have p-values that are smaller than the adopted significance level of $\alpha = 0.05$; and therefore, we can keep all of them in the model due to their potential contribution to the fit of the model.

Nonetheless, if we could not achieve a high enough accuracy and the classification performance was poor, we can take advantage of feature selection methods to solely select the features that perform better in the F-test, and remove the rest from the input features of our classification model. Moreover, we can also use the principal component analysis which has been shown to improve the accuracy of supervised learning models in special cases.

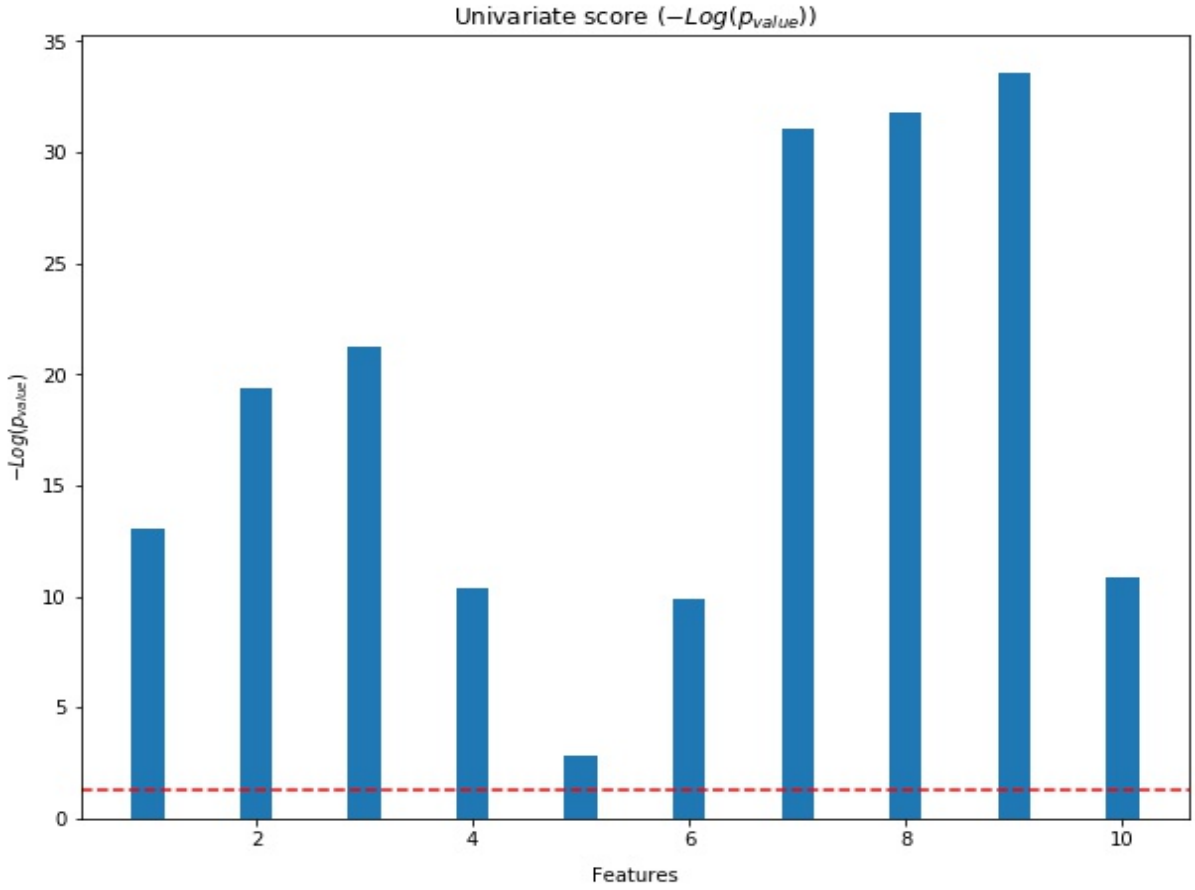

Figure 13: Significance of terminal input features

Ultimately, we train the classification models with the nine algorithms selected in this study and evaluate their accuracy. The highest accuracy reached in 94.4% which is even higher than the accuracy that we achieved for service legs. Table 13 shows a summary of accuracy values obtained from the nine classification algorithms implemented along with a visual representation of each model's confusion matrix. We elaborated on the significance and meaning of these accuracy values and confusion matrices in Section 6.2.1.

Table 16: Performance of classification models (terminals)

Support Vector Classifier	Neural Network	K-Nearest Neighbors
Accuracy: 94.4%	Accuracy: 94.4%	Accuracy: 94.4%
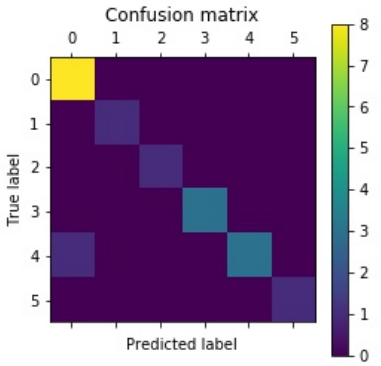	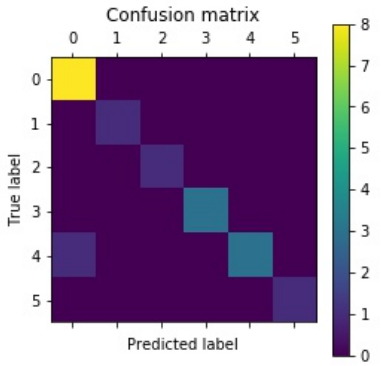	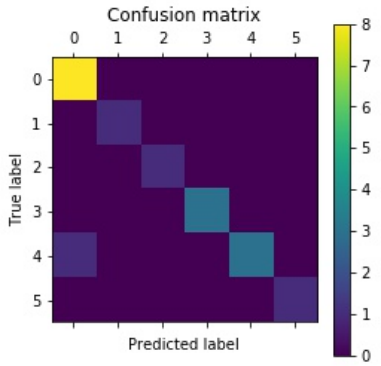
Decision Tree Classifier	**Random Forests**	**Bagging**
Accuracy: 88.8%	Accuracy: 88.8%	Accuracy: 94.4%
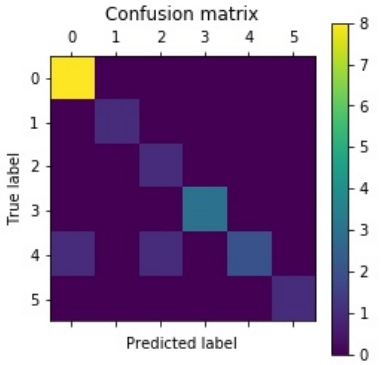	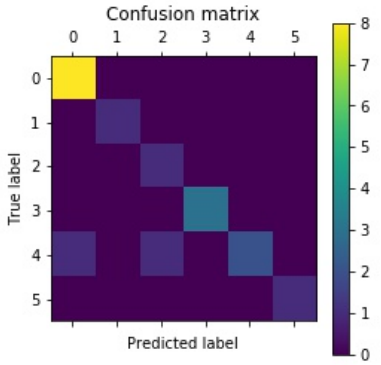	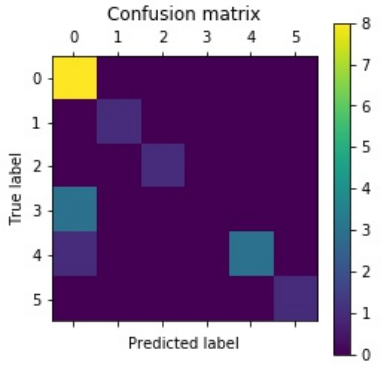
Gradient Boosting	**Linear Discriminant Analysis**	**Gaussian Naive Bayes**
Accuracy: 88.8%	Accuracy: 94.4%	Accuracy: 88.8%
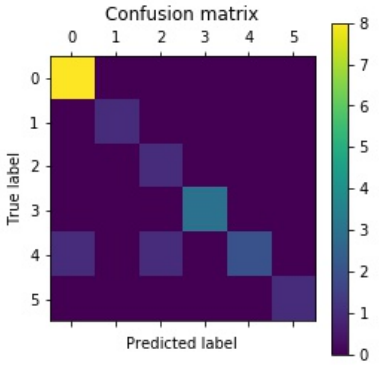	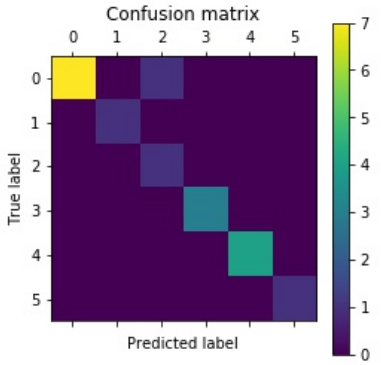	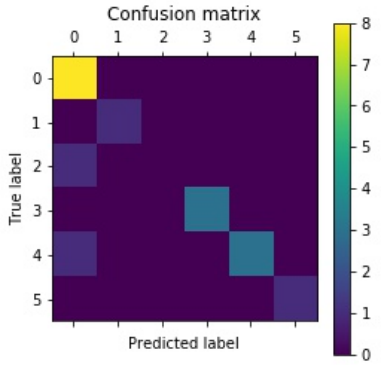

6.3 Validation of the classification models

In this section, we evaluate the performance of the classification models trained on data from the previous transportation periods on a new problem instance representing a new transportation period.

In order to test the validity of our methodology, we create a new shipment planning problem instance by generating new random demand data for each traffic-class, and solve the routing optimization model for the normal operating conditions of the network. Having obtained the optimal number of containers/trains utilizing each service leg or terminal from the optimal solution of the non-disruption case, we compile a data set of input features required to be able to make predictions using the previously trained classification models. Subsequently, we use the predictive model to assign the infrastructure to the previously defined criticality classes.

However, in order to be able to assess the accuracy of these predictions, we need to know every network element's actual criticality class which is based on how much the total cost/risk of operations increase in case this element is disrupted. Consequently, we solve the optimization model for every one of the disruption events individually and calculate the increase in total risk/cost compared with the non-disruption case for each of them. By inputting these

post-disruption cost/risk increases into the K-means clustering algorithm, we obtain the correct label (criticality class) for each service leg and terminal.

Comparing the aforementioned true labels with the predicted labels obtained from running the classification models on the new problem instance's feature data set provides us with the level of accuracy of each predictive classification model. Table 17 and Table 18 illustrate the performance of the nine previously trained classification models on the new problem instance for service legs and terminals respectively.

The highest accuracy achieved by a classification model for service legs belongs to support vector classifier and random forests in both the training/test data set with 93.3% accuracy and the validation data set with 92.5% accuracy. As for terminals, support vector classifier again performs best along with the k-nearest neighbors technique, with both achieving an accuracy of 94.4% on the training/test data set and an accuracy of 87.5% on the validation data set.

Based on these results, the proposed methodology can classify service legs with approximately 93% accuracy, in addition to classifying terminals with roughly 88% accuracy which are impressive results for a classification task. Therefore, we have validated our proposed methodology's capabilities in providing the company's managers with a valuable decision making tool that efficiently identifies critical infrastructure.

Table 17: Classification performance on validation data (service legs)

Support Vector Classifier	Neural Network	K-Nearest Neighbors
Accuracy: 92.5%	Accuracy: 88.8%	Accuracy: 88.8%
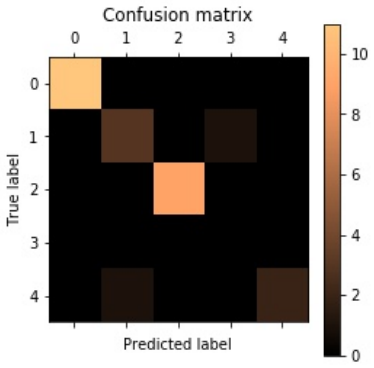	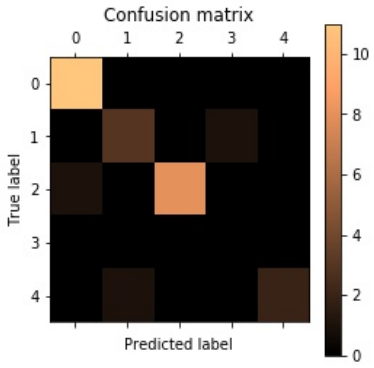	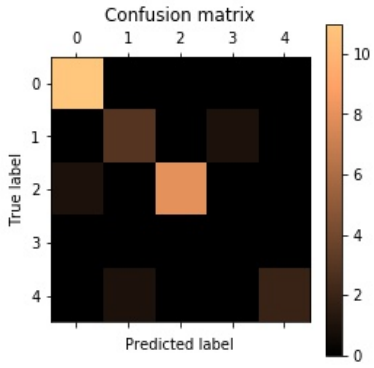
Decision Tree Classifier	**Random Forests**	**Bagging**
Accuracy: 88.8%	Accuracy: 92.5%	Accuracy: 92.5%
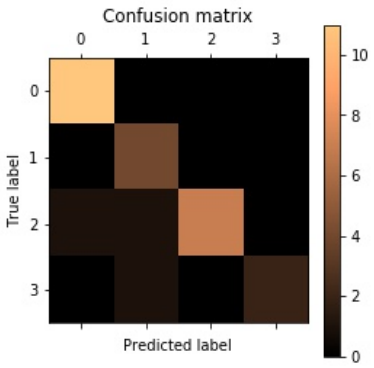	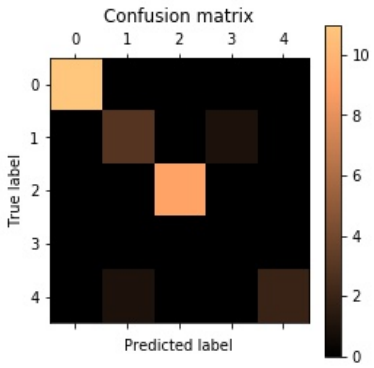	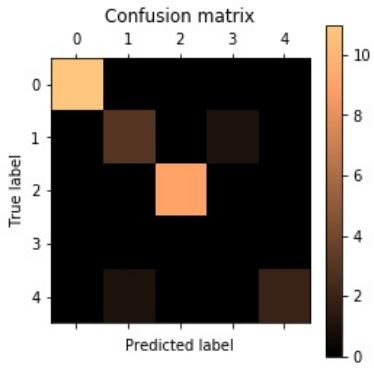
Gradient Boosting	**Linear Discriminant Analysis**	**Gaussian Naive Bayes**
Accuracy: 92.5%	Accuracy: 77.7%	Accuracy: 66.6%
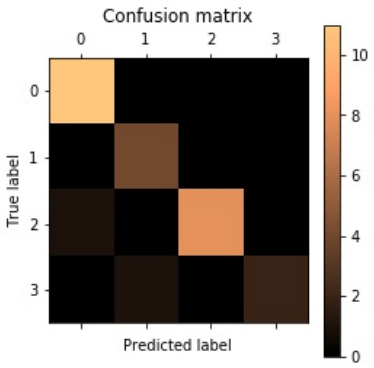	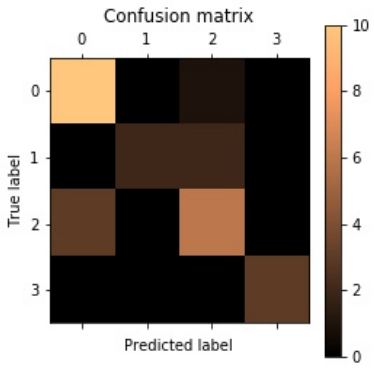	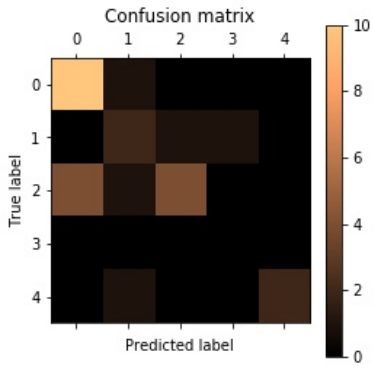

Table 18: Classification performance on validation data (terminals)

Support Vector Classifier	Neural Network	K-Nearest Neighbors
Accuracy: 87.5%	Accuracy: 75%	Accuracy: 87.5%
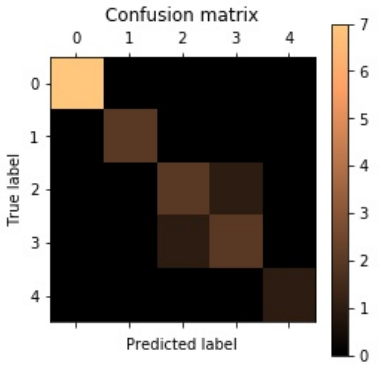	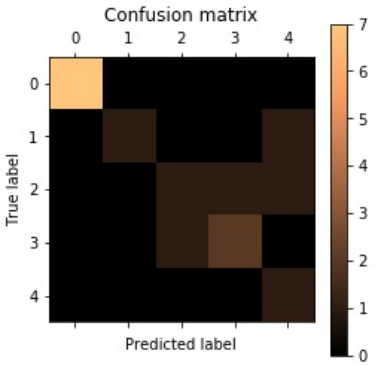	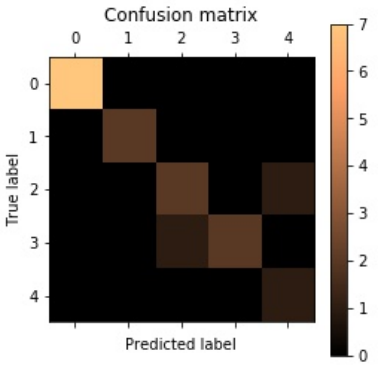
Decision Tree Classifier	**Random Forests**	**Bagging**
Accuracy: 75%	Accuracy: 81.2%	Accuracy: 81.2%
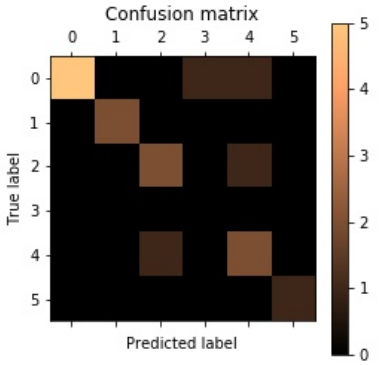	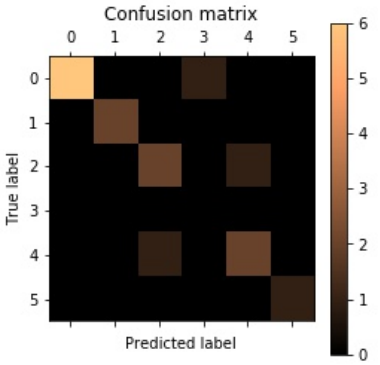	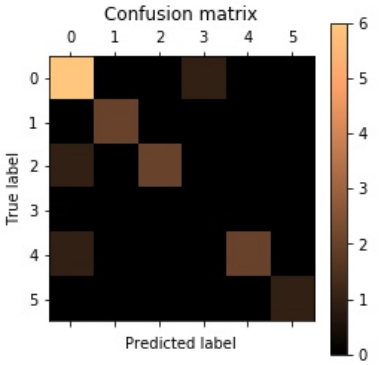
Gradient Boosting	**Linear Discriminant Analysis**	**Gaussian Naive Bayes**
Accuracy: 81.2%	Accuracy: 81.2%	Accuracy: 68.7%
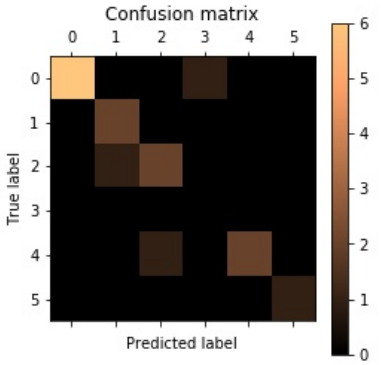	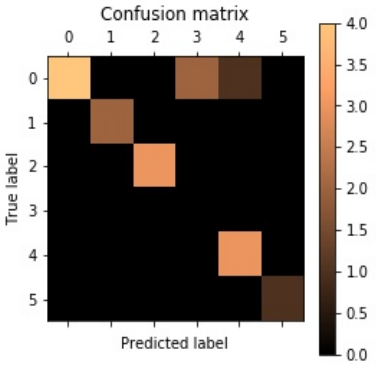	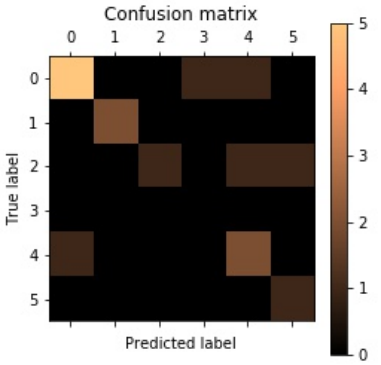

Figure 14 is a visual representation of the results of classification obtained from the support vector classifier algorithm for train service legs and intermodal terminals in the validation problem instance. The service legs represented by red lines are those that increase both cost and risk significantly. In other words, the classification model has classified these service legs in either of the Steep or High Cost & Risk Impact categories introduced in Table 8. The service legs drawn in yellow only increase the risk by a significant amount. This means that the classification model has classified them into the Steep Risk Impact category in Table 8. The rest of the service legs have been classified into the Moderate or Low Cost & Risk Impact category and are represented by green lines signifying lack of criticality.

As for the terminals, the red points represent the terminals whose disruption results in a significant increase in total cost; in other words, the Steep and High Cost Impact categories in Table 10. The yellow points represent the terminals causing a significant increase in post-disruption total risk, meaning the Steep and High Risk Impact categories. Lastly, the terminals represented by green points belong to the Moderate or Low Cost & Risk Impact categories.

Equipped with this knowledge of critical infrastructure, the company's managers can plan and apply mitigation strategies to the highest priority service legs and intermodal terminals in the network.

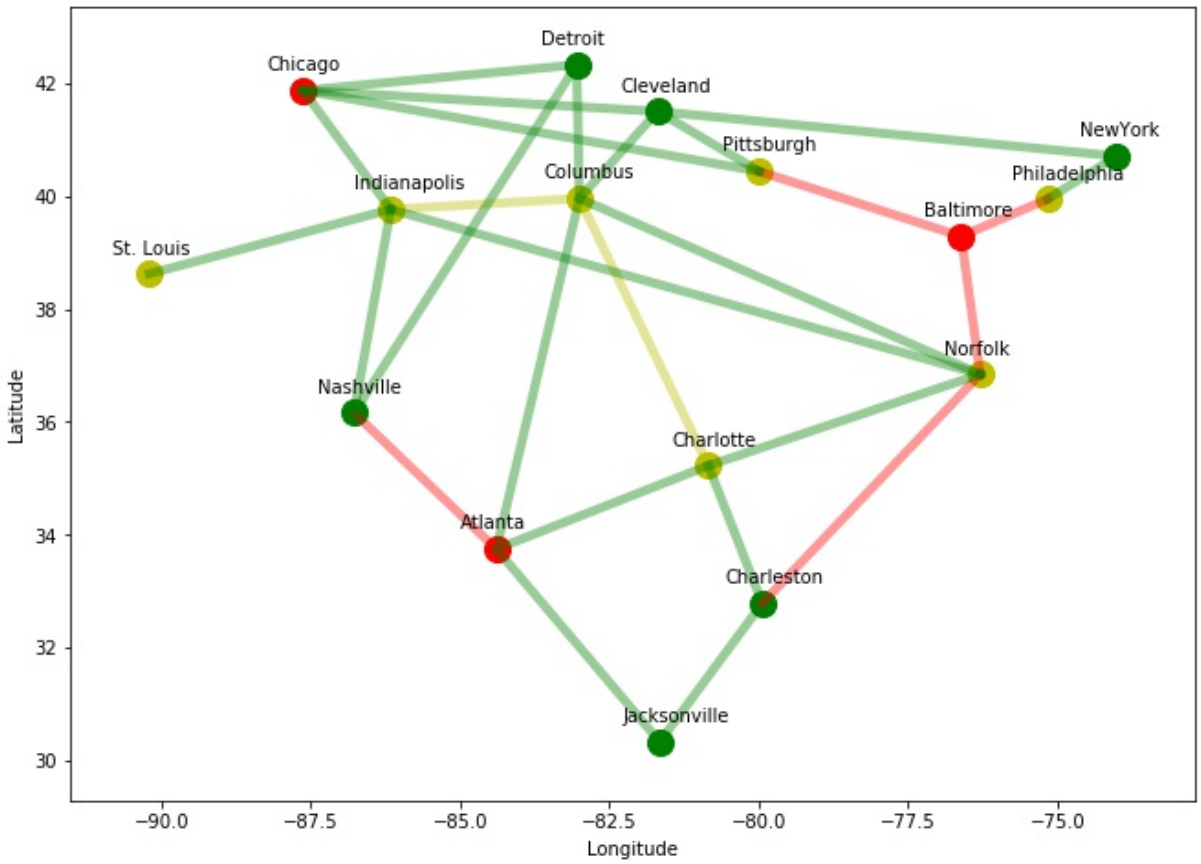

Figure 14: Critical service legs and terminals

For instance, all the service legs connected to the the Baltimore terminal have been identified as critical in terms of both the cost and the risk impact. Considering that the Baltimore terminal is identified to be critical in terms of cost impact and the terminals in Philadelphia, Pittsburgh and Norfolk are critical in terms of risk impact, decision makers should pay special attention to the network elements in this area. Furthermore, a problematic area in terms of post-disruption risk impact consists of service legs connecting Charlotte and Indianapolis to Columbus and the corresponding terminals.

Chapter 7

Conclusions

In this study, we introduced a decision making tool for the managers of rail-truck intermodal transportation companies in the form of a disruption risk mitigation methodology that can be used in the transportation planning of both regular and hazmat freight in networks with multiple terminals. The method utilizes a machine learning technique known as classification that makes predictions based on a set of input features extracted from inherent network attributes and topology, alongside a set of features obtained from the optimal shipment plan that represents the results of the presented bi-objective tactical routing optimization model.

The proposed methodology was applied to a case study of an intermodal rail-truck network in the north-east, south-east and mid-west regions of the US. We found that the methodology enables us to classify the network infras-

tructure with high accuracy both in the case of train service legs and in the case of terminals. The output of this methodology is the knowledge of the most critical network elements which assists transportation company managers to avoid significant surges in total cost and total risk of operations in case of a disruption event by implementing mitigation strategies in advance.

To the best of our knowledge, no other work in the literature provides an analytical framework for identifying critical train service legs and intermodal terminals by using bi-objective optimization as well as classification/clustering algorithms, in order to assist disruption risk mitigation efforts in hazardous material rail-truck intermodal transportation networks. We have contributed to the literature by developing a customized methodology of disruption risk mitigation that combines optimization modeling with supervised and unsupervised machine learning techniques in rail-truck intermodal networks which transport both regular freight and different classes of hazmat shipments.

Future research in this area may be done on the removal of the assumption regarding the availability of all train services when the transportation period begins and the incorporation of train service scheduling into the optimization model which increases its complexity. Future research may also be directed toward studying the inclusion of a direct trucking option in case of infeasibility of fulfilling demand due to multiple simultaneous disruptions.

References

AAR. (2018a). *Rail freight and intermodal*. American Association of Railroads. Retrieved February 1, 2020, from https://www.aar.org/wp-content/uploads/2018/03/AAR-Intermodal-Issue.pdf

AAR. (2018b). *Rail intermodal keeps america moving*. American Association of Railroads. Retrieved February 1, 2020, from https://www.aar.org/wp-content/uploads/2018/07/AAR-Rail-Intermodal.pdf

Abkowitz, M., Lepofsky, M., & Cheng, P. (1992). Selecting criteria for designating hazardous materials highway routes. *Transportation Research Record*, *1333*(2.2).

Alp, E. (1995). Risk-based transportation planning practice: Overall methodology and a case example. *INFOR: Information Systems and Operational Research*, *33*(1), 4–19.

Altazin, E., Dauzère-Pérès, S., Ramond, F., & Tréfond, S. (2020). A multi-objective optimization-simulation approach for real time rescheduling in dense railway systems. *European Journal of Operational Research*.

Asakura, Y. (1999). Reliability measures of an origin and destination pair in a deteriorated road network with variable flows, In *Transportation networks: Recent methodological advances. selected proceedings of the 4th euro transportation meetingassociation of european operational research societies*.

Assadipour, G., Ke, G. Y., & Verma, M. (2015). Planning and managing intermodal transportation of hazardous materials with capacity selection and congestion. *Transportation Research Part E: Logistics and Transportation Review*, *76*, 45–57.

Assadipour, G., Ke, G. Y., & Verma, M. (2016). A toll-based bi-level programming approach to managing hazardous materials shipments over an intermodal transportation network. *Transportation Research Part D: Transport and Environment*, *47*, 208–221.

Azad, N., Hassini, E., & Verma, M. (2016). Disruption risk management in railroad networks: An optimization-based methodology and a case study. *Transportation Research Part B: Methodological*, *85*, 70–88.

Bababeik, M., Khademi, N., & Chen, A. (2018). Increasing the resilience level of a vulnerable rail network: The strategy of location and allocation of emergency relief trains. *Transportation Research Part E: Logistics and Transportation Review*, *119*, 110–128.

Bababeik, M., Nasiri, M. M., Khademi, N., & Chen, A. (2017). Vulnerability evaluation of freight railway networks using a heuristic routing and scheduling optimization model. *Transportation*, 1–28.

Bagheri, M., Saccomanno, F., Chenouri, S., & Fu, L. (2011). Reducing the threat of in-transit derailments involving dangerous goods through effective placement along the train consist. *Accident Analysis & Prevention*, *43*(3), 613–620.

Batta, R., & Chiu, S. S. (1988). Optimal obnoxious paths on a network: Transportation of hazardous materials. *Operations research*, *36*(1), 84–92.

Bontekoning, Y. M., Macharis, C., & Trip, J. J. (2004). Is a new applied transportation research field emerging?—-a review of intermodal rail–truck freight transport literature. *Transportation research part A: Policy and practice*, *38*(1), 1–34.

Bornay, B., Chen, M., & Chauhan, S. (2020). Freight transportation planning for regular and hazmat materials with simplified risk functions. *Journal of Transportation Safety & Security*, 1–28.

BTS. (2017). *Freight facts and figures 2017*. U.S. Department of Transportation, Bureau of Transportation Statistics. Retrieved February 1, 2020, from https://www.bts.gov/newsroom/freight-facts-and-figures-2017

BTS, & FHWA. (2018). *Freight analysis framework, version 4.4.1.* U.S. Department of Transportation, Bureau of Transportation Statistics and Federal Highway Administration. Retrieved February 1, 2020, from https://www.bts.gov/faf

Bubbico, R., Di Cave, S., & Mazzarotta, B. (2004). Risk analysis for road and rail transport of hazardous materials: A gis approach. *Journal of Loss prevention in the Process Industries*, *17*(6), 483–488.

Bubbico, R., Maschio, G., Mazzarotta, B., Milazzo, M. F., & Parisi, E. (2006). Risk management of road and rail transport of hazardous materials in sicily. *Journal of Loss Prevention in the Process Industries*, *19*(1), 32–38.

Burgholzer, W., Bauer, G., Posset, M., & Jammernegg, W. (2013). Analysing the impact of disruptions in intermodal transport networks: A micro simulation-based model. *Decision Support Systems*, *54*(4), 1580–1586.

Cacchiani, V., Huisman, D., Kidd, M., Kroon, L., Toth, P., Veelenturf, L., & Wagenaar, J. (2014). An overview of recovery models and algorithms for real-time railway rescheduling. *Transportation Research Part B: Methodological*, *63*, 15–37.

CBC. (2020). *Rail blockades causing containers to pile up at canadian ports*. Canadian Broadcasting Corporation. Retrieved February 1, 2020, from https://www.cbc.ca/news/business/rail-blockade-ports-1.5471312

Chen, A., Yang, H., Lo, H. K., & Tang, W. H. (2002). Capacity reliability of a road network: An assessment methodology and numerical results. *Transportation Research Part B: Methodological*, *36*(3), 225–252.

Chen, L., & Miller-Hooks, E. (2012). Resilience: An indicator of recovery capability in intermodal freight transport. *Transportation Science*, *46*(1), 109–123.

Cordeiro, F. G., Bezerra, B. S., Peixoto, A. S. P., & Ramos, R. A. R. (2016). Methodological aspects for modeling the environmental risk of transporting hazardous materials by road. *Transportation research part D: transport and environment*, *44*, 105–121.

CSX. (2020a). *Hazardous commodities by u.s. dot classification*. CSX Corporation. Retrieved August 30, 2020, from https://www.csx.com/index.cfm/about-us/safety/hazardous-materials1/hazardous-commodities-by-u-s-dot-classification/

CSX. (2020b). *Performance measures*. CSX Corporation. Retrieved May 30, 2020, from https://www.csx.com/index.cfm/customers/performance-measures/#Data

Deb, K. (2001). *Multi-objective optimization using evolutionary algorithms* (Vol. 16). John Wiley & Sons.

EPA. (2016, September). *ALOHA* (Version 5.4.7). https://www.epa.gov/cameo/aloha-software

Erkut, E., & Ingolfsson, A. (2000). Catastrophe avoidance models for hazardous materials route planning. *Transportation Science*, *34*(2), 165–179.

Erkut, E., Tjandra, S. A., & Verter, V. (2007). Hazardous materials transportation. *Handbooks in operations research and management science*, *14*, 539–621.

Erkut, E., & Verter, V. (1995). A framework for hazardous materials transport risk assessment. *Risk Analysis*, *15*(5), 589–601.

Erkut, E., & Verter, V. (1998). Modeling of transport risk for hazardous materials. *Operations research*, *46*(5), 625–642.

ESRI. (2020, February 20). *ArcGIS Pro* (Version 10.8). https://www.esri.com/en-us/arcgis/products/arcgis-pro/overview

Faghih-Roohi, S., Ong, Y.-S., Asian, S., & Zhang, A. N. (2016). Dynamic conditional value-at-risk model for routing and scheduling of hazardous material transportation networks. *Annals of Operations Research*, *247*(2), 715–734.

Faturechi, R., & Miller-Hooks, E. (2015). Measuring the performance of transportation infrastructure systems in disasters: A comprehensive review. *Journal of infrastructure systems*, *21*(1), 04014025.

Fikar, C., Hirsch, P., Posset, M., & Gronalt, M. (2016). Impact of transalpine rail network disruptions: A study of the brenner pass. *Journal of Transport Geography*, *54*, 122–131.

FMCSA. (2001). *Comparative risks of hazardous materials and non-hazardous materials truck shipment accidents/incidents*. Federal Motor Carrier Safety Administration. Retrieved August 30, 2020, from https://www.hsdl.org/?abstract&did=233019

Ghaderi, A., & Burdett, R. L. (2019). An integrated location and routing approach for transporting hazardous materials in a bi-modal transportation network. *Transportation research part E: logistics and transportation review*, *127*, 49–65.

Glickman, T. S. (1983). Rerouting railroad shipments of hazardous materials to avoid populated areas. *Accident Analysis & Prevention*, *15*(5), 329–335.

Glickman, T. S., Erkut, E., & Zschocke, M. S. (2007). The cost and risk impacts of rerouting railroad shipments of hazardous materials. *Accident Analysis & Prevention*, *39*(5), 1015–1025.

Grodzevich, O., & Romanko, O. (2006). Normalization and other topics in multi-objective optimization.

Gu, Y., Fu, X., Liu, Z., Xu, X., & Chen, A. (2020). Performance of transportation network under perturbations: Reliability, vulnerability, and resilience. *Transportation Research Part E: Logistics and Transportation Review*, *133*, 101809.

Gurobi Optimization, L. (2020). Gurobi optimizer reference manual. http://www.gurobi.com

Holeczek, N. (2019). Hazardous materials truck transportation problems: A classification and state of the art literature review. *Transportation research part D: transport and environment*, *69*, 305–328.

Hosseini, S. D., & Verma, M. (2017). A value-at-risk (var) approach to routing rail hazmat shipments. *Transportation research part D: transport and environment*, *54*, 191–211.

Hosseini, S. D., & Verma, M. (2018). Conditional value-at-risk (cvar) methodology to optimal train configuration and routing of rail hazmat shipments. *Transportation Research Part B: Methodological*, *110*, 79–103.

Huang, M., Hu, X., & Zhang, L. (2011). A decision method for disruption management problems in intermodal freight transport. In *Intelligent decision technologies* (pp. 13–21). Springer.

Ishfaq, R. (2012). Resilience through flexibility in transportation operations. *International Journal of Logistics Research and Applications*, *15*(4), 215–229.

Jabbarzadeh, A., Azad, N., & Verma, M. (2019). An optimization approach to planning rail hazmat shipments in the presence of random disruptions. *Omega*, 102078.

Jafino, B. A., Kwakkel, J., & Verbraeck, A. (2020). Transport network criticality metrics: A comparative analysis and a guideline for selection. *Transport Reviews*, *40*(2), 241–264.

James, G., Witten, D., Hastie, T., & Tibshirani, R. (2013). *An introduction to statistical learning* (Vol. 112). Springer.

Jenelius, E., Petersen, T., & Mattsson, L.-G. (2006). Importance and exposure in road network vulnerability analysis. *Transportation Research Part A: Policy and Practice*, *40*(7), 537–560.

Kang, Y., Batta, R., & Kwon, C. (2014a). Generalized route planning model for hazardous material transportation with var and equity considerations. *Computers & Operations Research*, *43*, 237–247.

Kang, Y., Batta, R., & Kwon, C. (2014b). Value-at-risk model for hazardous material transportation. *Annals of Operations Research*, *222*(1), 361–387.

Ke, G. Y. (2020). Managing rail-truck intermodal transportation for hazardous materials with random yard disruptions. *Annals of Operations Research*, 1–27.

Khaled, A. A., Jin, M., Clarke, D. B., & Hoque, M. A. (2015). Train design and routing optimization for evaluating criticality of freight railroad infrastructures. *Transportation Research Part B: Methodological*, *71*, 71–84.

List, G. F., Mirchandani, P. B., Turnquist, M. A., & Zografos, K. G. (1991). Modeling and analysis for hazardous materials transportation: Risk analysis, routing/scheduling and facility location. *Transportation Science*, *25*(2), 100–114.

Machado, E. R., do Valle Júnior, R. F., Fernandes, L. F. S., & Pacheco, F. A. L. (2018). The vulnerability of the environment to spills of dangerous substances on highways: A diagnosis based on multi criteria modeling. *Transportation research part D: transport and environment*, *62*, 748–759.

Martıénez-Alegrıéa, R., Ordóñez, C., & Taboada, J. (2003). A conceptual model for analyzing the risks involved in the transportation of hazardous goods: Implementation in a geographic information system. *Human and Ecological Risk Assessment*, *9*(3), 857–873.

Mattsson, L.-G., & Jenelius, E. (2015). Vulnerability and resilience of transport systems–a discussion of recent research. *Transportation Research Part A: Policy and Practice*, *81*, 16–34.

Mazzarotta, B. (2002). Risk reduction when transporting dangerous goods: Road or rail? *Risk, Decision and Policy*, *7*(1), 45–56.

Miller-Hooks, E., Zhang, X., & Faturechi, R. (2012). Measuring and maximizing resilience of freight transportation networks. *Computers & Operations Research*, *39*(7), 1633–1643.

Nicholson, A., & Du, Z.-P. (1997). Degradable transportation systems: An integrated equilibrium model. *Transportation Research Part B: Methodological*, *31*(3), 209–223.

Nozick, L. K., & Morlok, E. K. (1997). A model for medium-term operations planning in an intermodal rail-truck service. *Transportation research part a: policy and practice*, *31*(2), 91–107.

Pedregosa, F., Varoquaux, G., Gramfort, A., Michel, V., Thirion, B., Grisel, O., Blondel, M., Prettenhofer, P., Weiss, R., Dubourg, V., Vanderplas, J., Passos, A., Cournapeau, D., Brucher, M., Perrot, M., & Duchesnay, E. (2011). Scikit-learn: Machine learning in Python. *Journal of Machine Learning Research*, *12*, 2825–2830.

Peterson, S. K., & Church, R. L. (2008). A framework for modeling rail transport vulnerability. *Growth and Change*, *39*(4), 617–641.

PHMSA. (2020a). *Hazardous materials regulations*. Pipeline and Hazardous Materials Safety Administration. Retrieved February 1, 2020, from https://www.phmsa.dot.gov/standards-rulemaking/hazmat/hazardous-materials-regulations

PHMSA. (2020b). *Hazmat incident database*. Pipeline and Hazardous Materials Safety Administration. Retrieved February 1, 2020, from https://www.phmsa.dot.gov/hazmat-program-management-data-and-statistics/data-operations/incident-statistics

ReVelle, C., Cohon, J., & Shobrys, D. (1991). Simultaneous siting and routing in the disposal of hazardous wastes. *Transportation Science*, *25*(2), 138–145.

Saat, M. R., Werth, C. J., Schaeffer, D., Yoon, H., & Barkan, C. P. (2014). Environmental risk analysis of hazardous material rail transportation. *Journal of hazardous materials*, *264*, 560–569.

Saccomanno, F. F., & Chan, A.-W. (1985). *Economic evaluation of routing strategies for hazardous road shipments*.

Sarhadi, H., Tulett, D. M., & Verma, M. (2017). An analytical approach to the protection planning of a rail intermodal terminal network. *European Journal of Operational Research*, *257*(2), 511–525.

Sato, K., & Fukumura, N. (2012). Real-time freight locomotive rescheduling and uncovered train detection during disruption. *European Journal of Operational Research*, *221*(3), 636–648.

Scott, D. M., Novak, D. C., Aultman-Hall, L., & Guo, F. (2006). Network robustness index: A new method for identifying critical links and evaluating the performance of transportation networks. *Journal of Transport Geography*, *14*(3), 215–227.

Sohn, J. (2006). Evaluating the significance of highway network links under the flood damage: An accessibility approach. *Transportation research part A: policy and practice*, *40*(6), 491–506.

SteadieSeifi, M., Dellaert, N. P., Nuijten, W., Van Woensel, T., & Raoufi, R. (2014). Multimodal freight transportation planning: A literature review. *European journal of operational research*, *233*(1), 1–15.

Stecke, K. E., & Kumar, S. (2009). Sources of supply chain disruptions, factors that breed vulnerability, and mitigating strategies. *Journal of Marketing Channels*, *16*(3), 193–226.

Su, L., Sun, L., Karwan, M., & Kwon, C. (2019). Spectral risk measure minimization in hazardous materials transportation. *IISE Transactions*, *51*(6), 638–652.

Sullivan, J., Aultman-Hall, L., & Novak, D. (2009). A review of current practice in network disruption analysis and an assessment of the ability to account for isolating links in transportation networks. *Transportation Letters*, *1*(4), 271–280.

Sullivan, J., Novak, D. C., Aultman-Hall, L., & Scott, D. M. (2010). Identifying critical road segments and measuring system-wide robustness in transportation networks with isolating links: A link-based capacity-reduction approach. *Transportation Research Part A: Policy and Practice*, *44*(5), 323–336.

Toumazis, I., & Kwon, C. (2013). Routing hazardous materials on time-dependent networks using conditional value-at-risk. *Transportation Research Part C: Emerging Technologies*, *37*, 73–92.

Toumazis, I., & Kwon, C. (2016). Worst-case conditional value-at-risk minimization for hazardous materials transportation. *Transportation Science*, *50*(4), 1174–1187.

Toumazis, I., Kwon, C., & Batta, R. (2013). Value-at-risk and conditional value-at-risk minimization for hazardous materials routing. In *Handbook of or/ms models in hazardous materials transportation* (pp. 127–154). Springer.

TSB. (2019). *Railway investigation report r13d0054*. Transportation Safety Board of Canada. Retrieved February 1, 2020, from https://www.tsb.gc.ca/eng/rapports-reports/rail/2013/r13d0054/r13d0054-r-es.html

Uddin, M., & Huynh, N. (2016). Routing model for multicommodity freight in an intermodal network under disruptions. *Transportation Research Record*, *2548*(1), 71–80.

Uddin, M., & Huynh, N. (2019). Reliable routing of road-rail intermodal freight under uncertainty. *Networks and Spatial Economics*, *19*(3), 929–952.

Vaezi, A. (2018). *Risk mitigation and management strategies for routing hazardous materials over railroad network in canada* (Doctoral dissertation).

Veelenturf, L. P., Kidd, M. P., Cacchiani, V., Kroon, L. G., & Toth, P. (2016). A railway timetable rescheduling approach for handling large-scale disruptions. *Transportation Science*, *50*(3), 841–862.

Verma, M. (2009). A cost and expected consequence approach to planning and managing railroad transportation of hazardous materials. *Transportation research part D: transport and environment*, *14*(5), 300–308.

Verma, M. (2011). Railroad transportation of dangerous goods: A conditional exposure approach to minimize transport risk. *Transportation research part C: emerging technologies*, *19*(5), 790–802.

Verma, M., & Verter, V. (2007). Railroad transportation of dangerous goods: Population exposure to airborne toxins. *Computers & operations research*, *34*(5), 1287–1303.

Verma, M., & Verter, V. (2008). The trade-offs in rail-truck intermodal transportation of hazardous materials: An illustrative case study. *Advanced Technologies and Methodologies for Risk Management in the Global Transport of Dangerous Goods: NATO Science for Peace and Security Series*, *45*, 148–168.

Verma, M., & Verter, V. (2010). A lead-time based approach for planning rail–truck intermodal transportation of dangerous goods. *European Journal of Operational Research*, *202*(3), 696–706.

Verma, M., & Verter, V. (2013). Railroad transportation of hazardous materials: Models for risk assessment and management. In *Handbook of or/ms models in hazardous materials transportation* (pp. 9–47). Springer.

Verma, M., Verter, V., & Gendreau, M. (2011). A tactical planning model for railroad transportation of dangerous goods. *Transportation science*, *45*(2), 163–174.

Verma, M., Verter, V., & Zufferey, N. (2012). A bi-objective model for planning and managing rail-truck intermodal transportation of hazardous materials. *Transportation research part E: logistics and transportation review*, *48*(1), 132–149.

Whitman, M. G., Barker, K., Johansson, J., & Darayi, M. (2017). Component importance for multi-commodity networks: Application in the swedish railway. *Computers & Industrial Engineering*, *112*, 274–288.

Xie, Y., Lu, W., Wang, W., & Quadrifoglio, L. (2012). A multimodal location and routing model for hazardous materials transportation. *Journal of hazardous materials*, *227*, 135–141.

Zhu, Y., & Goverde, R. M. (2019). Railway timetable rescheduling with flexible stopping and flexible short-turning during disruptions. *Transportation Research Part B: Methodological*, *123*, 149–181.

Zografos, K. G., & Androutsopoulos, K. N. (2004). A heuristic algorithm for solving hazardous materials distribution problems. *European Journal of Operational Research*, *152*(2), 507–519.